Am J Cancer Res 2024;14(12):6012-6036
www.ajcr.us /ISSN:2156-6976/ajcr0160173

Original Article

Synergistic combination therapy with ONC201 or ONC206, and enzalutamide or darolutamide in preclinical studies of castration-resistant prostate cancer

Laura Jinxuan Wu[1,2], Maximilian Pinho-Schwermann[1,3,7], Lanlan Zhou[1,3,4,7], Leiqing Zhang[1,4,7], Kelsey E Huntington[1,5,7], Ryan Malpass[1,7], Attila A Seyhan[1,3,4,7], Benedito A Carneiro[1,3,6,7], Wafik S El-Deiry[1,3,4,5,6,7]

[1]Laboratory of Translational Oncology and Experimental Cancer Therapeutics, The Warren Alpert Medical School, Brown University, Providence, RI 02903, USA; [2]Biotechnology Graduate Program, Brown University, Providence, RI 02903, USA; [3]The Joint Program in Cancer Biology, Brown University and The Lifespan Health System, Providence, RI 02903, USA; [4]Department of Pathology and Laboratory Medicine, The Warren Alpert Medical School, Brown University, Providence, RI 02903, USA; [5]Pathobiology Graduate Program, The Warren Alpert Medical School, Brown University, Providence, RI 02903, USA; [6]Hematology-Oncology Division, Department of Medicine, Rhode Island Hospital and Brown University, Providence, RI 02903, USA; [7]Legorreta Cancer Center at Brown University, The Warren Alpert Medical School, Brown University, Providence, RI 02903, USA

Received August 29, 2024; Accepted November 10, 2024; Epub December 25, 2024; Published December 30, 2024

Abstract: Androgen receptor (AR) signaling is a target in prostate cancer therapy and can be treated with non-steroidal anti-androgens (NSAA) including enzalutamide, and apalutamide for patients with advanced disease. Metastatic castration-resistant prostate cancer (mCPRC) develop resistance becomes refractory to therapy limiting patient overall survival. Darolutamide is a novel next-generation androgen receptor-signaling inhibitor that is FDA approved for non-metastatic castration resistant prostate cancer (nmCRPC). Imipridone ONC201/TIC10 is first-in-class small molecule imipridone that activates the integrated stress response (ISR), upregulates TNF-related apoptosis-inducing ligand (TRAIL) and has activity against CRPC alone or in combination with enzalutamide in preclinical models. We hypothesized that combination of imipridones with androgen receptor signaling blockers such as darolutamide may synergize in anti-tumor efficacy against mCRPC cells. mCRPC cell lines 22RV1, LNCaP, DU145 and PC3 were treated with imipridones ONC201, ONC206, apalutamide, darolutamide, or enzalutamide as single agents or in combinations. Combinations of ONC201 or ONC206 and androgen receptor signaling blockers demonstrated synergistic effects in mCRPC cells. Combinations of ONC201 and darolutamide or enzalutamide reduced PSA levels in LNCaP cells and induced of ATF4 in both LNCaP and 22RV1 cell lines. Darolutamide synergized with ONC201 regardless of AR status or castration sensitivity *in vitro*. Flow cytometric analysis showed increased intra-tumoral NK cells in mice treated with ONC201 and combination of ONC201 and darolutamide. Trends of increased TRAIL activation within NK cells were also observed in treatment groups. ONC201 and darolutamide demonstrated anti-tumor effects *in vivo* in the 22RV1 CRPC model. Our results prompt further translational and clinical studies with imipridones ONC201 or ONC206 in combination with enzalutamide or darolutamide for treatment of castrate resistant advanced or metastatic prostate cancer.

Keywords: Prostate cancer, ONC201, ONC206, enzalutamide, darolutamide, castrate resistance

Introduction

Advanced metastatic castrate resistant prostate cancer remains challenging to treat especially among elderly patients with bone or organ metastases [1, 2]. While most advanced prostate cancer is androgen-sensitive at diagnosis and treatable with androgen deprivation, therapeutic resistance occurs [3, 4]. In the last 10-15 years, targeting androgen receptor signaling has been possible with AR pathway signaling inhibitors such as enzalutamide, apalutamide and darolutamide or androgen synthesis inhibition such as with abiraterone [5-7]. A subset of

https://doi.org/10.62347/VJMW4904

patients with prostate cancer have underlying molecular pathology involving loss of BRCA2 or other homologous recombination defects and those patients can be treated with PARP inhibitors as well as combinations that include PARP inhibition [8]. Other molecular defects such as PTEN loss or mutation, PIK3CA or Akt1/2/3 mutation have therapeutics under development. Gene fusions such as the ETS gene fusion TMPRSS2-ERG and mutations on p53, Rb, SPOP, CDK12 deletion and microsatellite instability have been described [9, 10]. Castrate-resistant prostate cancer becomes refractory to therapeutics, including a major subset that undergoes neuroendocrine differentiation, and these tumors need novel effective therapeutic strategies [11-16].

Our laboratory previously discovered and reported TRAIL-Inducing Compound #10 (TIC10) as a first-in-class anticancer agent [17]. The drug (imipridone TIC10/ONC201) advanced to first-in-human clinical trials in solid tumors as well as brain tumors through Oncoceutics, Inc. [18] and more recently through Chimerix, Inc. [19, 20] that is conducting trials including a large phase III trial (ACTION study) in H3K27M-mutated diffuse midline glioma [21]. There are also ongoing early phase trials with ONC201 analogue ONC206 in brain tumors (NCT047-32065, NCT04541082).

The first-in-human study of ONC201 conducted by Stein *et al*. observed that a number of patients with advanced prostate cancer with bone or soft tissue metastases experienced reduction in tumor size and improvement in symptoms [18, 22]. Some of the patients with prostate cancer were over the age of 90. Of 8 patients with advance prostate cancer who were treated with ONC201, 5 remained on therapy for greater than 6 months indicating an early signal of drug activity in this disease. We previously discovered stimulation of natural killer cell activation by ONC201 [23]. A follow-up to the first-in-human ONC201 solid tumor study showed an association with immune biomarkers and prolonged disease-free survival in patients with solid tumors who were treated with ONC201 [22]. To date in 2024, there has not been a phase II study of ONC201, any of its analogues, or combinations with other cancer therapies in the treatment of prostate cancer.

We previously explored combination treatments with ONC201 such as everolimus or enzalutamide [24]. Although the combination of ONC201 and everolimus showed potent synergy including *in vivo*, there was little interest to move this combination to the clinic as mTOR inhibitors such as everolimus have not shown clinical activity in prostate cancer. As ONC201 has shown responses in non-H3K27M-mutated non-brain tumors such as neuroendocrine tumors (pheochromocytomas, paragangliomas) [25], and since neuroendocrine differentiation is a feature of castrate-resistant advanced prostate cancer, we became interested in exploring ONC201 and combinations with AR signaling inhibitors in prostate cancer. We had not previously conducted *in vivo* studies with ONC201 and enzalutamide and had not previously published studies of the combination of ONC201 or any imipridone plus darlolutamide in cell culture or *in vivo* [24].

In the present manuscript we further investigated combinations of ONC201 with enzalutamide as well as darolutamide including immunomodulatory and *in vivo* therapeutic effects in mice. We focused on darolutamide due to more favorable CNS toxicity profile for combination therapy with imipridones. Our results support the further clinical translation of imipridones such as ONC201 or ONC206 in combination with enzalutamide or darolutamide.

Material and methods

Cell culture and reagents

Human prostate cancer cells lines, LNCaP, 22RV1, DU145 and PC3 were obtained from the American Type Culture Collection (ATCC). The cell lines are maintained in RPMI-1640 medium with L-glutamine (HyClone, Cytiva Life Sciences) with an addition of 10% FBS and 1% penicillin-streptomycin solution and were routinely essayed for mycoplasma contamination. ONC201 and ONC206 were obtained from Chimerix, Inc. Enzalutamide was purchased from MedKoo Biosciences (Cat. no. 201821). Darolutamide was purchased from MedKoo Biosciences (Cat. no. 206514). Apalutamide was purchased from Selleck Chemicals (Cat. no. S2840). DHT was purchased from ApexBio (Cat. no. S8214). The compounds were dissolved in DMSO at 20 mmol/mL concentration and stored at -20°C.

CellTiter-Glo® luminescent cell viability assay

The CellTiter-Glo® (CTG) reagent is obtained from Promega and stored in -80°C to preserve

maximum light signal and other functional performances including half-life, linearity, and sensitivity. The CTG reagent was thawed at 4°C overnight or in a 22°C water bath and mixed gently before use per manufacturer's instructions (Promega). A total of 5000 prostate cancer cells per well were seeded in an opaque-walled 96-well plate. After incubation for 24 hours at 37°C, cells were treated with ONC201 (0.313, 0.625, 1.25, 2.5, 5 and 10 μmol/L), ONC206 (0.313, 0.625, 1.25, 2.5, 5 μmol/L), enzalutamide (0.313, 0.625, 1.25, 2.5, 5, 10, 20 and 40 or 80 μmol/L), darolutamide (0.313, 0.625, 1.25, 2.5, 5, 10, and 20, 40 or 80 μmol/L), or apalutamide (0.313, 0.625, 1.25, 2.5, 5, 10, 20, 40 and 80 μmol/L), as single agents or in combinations. Matched volumes of medium without drug additions were added as vehicle control. After 72 hours of incubation at 37°C, the viability of cells was measured. 20 μl of CTG reagent was added to each well containing 100 μl of cell and medium mixture. The content in the plate was mixed for at least 2 minutes on an orbital shaker. Luminescence was measured using the IVIS Xenogen 200 imaging system and cell viability was recorded. All single treatment groups and combinations were performed in triplicates. Results were reported as mean values ± SD of the percentage of cell viability. Dose response curves were generated and the half-maximum growth inhibitory concentration (IC50) for each single treatment group was calculated using GraphPad Prism version 9.3.0.

Drug combination and synergy data analysis

Combination indices were calculated using the CompuSyn software (ComboSyn Inc.). Heat maps showing the combination indices (CI) were made by excel with combination indices indicating synergy highlighted in yellow. Heat maps showing synergy verses antagonism were generated using Combenefit software (Combenefit™). Data generated from combination assays were processed using the Highest Single Agent (HSA) classical synergy model as single experiments. A model-based combination dose-response surface based on the two single agent dose-response curves was generated to determine any additive or non-synergistic combination. Heat maps showing synergy and antagonism distribution was then developed by comparing the model-generated combination dose response surface to the experimental one. The sets of metrics provided by the Combenefit software were then used to interpret synergy or antagonism.

Immunoblotting

Prostate cancer cells were maintained in RPMI 1640 medium with L-glutamine (HyClone, Cytiva Life Sciences) supplemented with 10% FBS and 1% penicillin-streptomycin. A total of 2.5-3 × 10^5 were seeded in medium and incubated overnight at 37°C with 5% CO_2 before treatment. After treatment, cells were washed with PBS and lysed with RIPA buffer (Cell Signaling) supplemented with one tablet of Complete™ EDTA-free protease inhibitor cocktail (Sigma-Aldrich) and one tablet of Halt™ phosphatase inhibitor (Thermo Fisher Scientific). The protein concentrations of the cell lysates were quantified using the BCA assay. To denature proteins, LDS sample buffer (Thermo Fisher Scientific) with 2% beta-mercaptoethanol was added and samples were placed on a heating block for 10 minutes. Equal amounts of proteins were then loaded into the 1.5 mm, 15 well NuPAGE 4-12% Bis-Tris gel (Thermo Fisher Scientific) and BLUEstain™ Protein ladder (Goldbio) was used as a molecular weight marker. Gels were run using 1× MES running buffer [prepared from 20× MES (Thermo Fisher Scientific)] at 0.4 A for 40 minutes. Separated proteins were then transferred to nitrocellulose membranes using wet transfer at 0.25 A for 1.5 hours. After blocking with 5% milk dissolved in TBS containing 0.1% Tween-20 for 30 minutes at room temperature, the membranes were incubated in primary antibodies diluted in 5% milk in TBS containing 0.1% Tween-20 (ATF4, cleaved-caspase 3 and PSA at 1:1000; cleaved-PARP at 1:2000; Ran at 1:5000) at 4°C overnight. After washing with 3 times with TTBS, membranes were incubated in appropriate secondary antibodies conjugated with horseradish peroxidase (goat anti-mouse IgG at 1:5000; goat anti-rabbit IgG at 1:10,000) for 1 hour at room temperature. Appropriate ECL reagents (Thermo Fisher Scientific) were added to the membranes for chemiluminescence detection using the Syngene Gel & Blot imaging system (SDI Group plc). The primary antibodies used in this study are as follows: antibodies against cleaved-PARP (Cell Signaling, cat. no. 9546s), AR (Cell Signaling, cat. no. 5153s), AR-V7 (Cell Signaling, cat. no. 68492s), cleaved caspase 3 (Cell Signaling, cat. no. 9661s), PSA/KLK3 (Cell

Signaling, cat. no. 2474s), ATF4 (Cell Signaling, cat. no. 11815s) and Ran (BD Biosciences cat. no. BD 610341). The secondary antibodies used in this study were obtained from Thermo Fisher Scientific [goat anti-mouse IgG (H+L) 31430 and goat anti-rabbit IgG (H+L) 31460].

Establishment of luciferase expressing human prostate cancer cell lines

Luciferase expressing prostate cancer cell line 22RV1-LUC was established to monitor mouse tumor growth by whole-body bioluminescence imaging using the IVIS Xenogen imaging system. 22RV1 prostate cancer cells were maintained at 60-70% confluency in RPMI 1640 medium with L-glutamine (HyClone, Cytiva Life Sciences) supplemented with 10% FBS and 1% penicillin-streptomycin. HEK293T cells were regularly maintained in DMEM/F12 1:1 medium with L-glutamine (Cytiva, cat. no. SH300-23.01) supplemented with 10% FBS and ABX. A total of 6-7 × 10^6 cells were seeded in medium and incubated overnight at 37°C with 5% CO_2 and were maintained at 60-70% confluency prior to transfection. Transfection mix was made using psPAX2/Helper packaging plasmid (Addgene, cat. no. 12260), pMD2.G/VSVG.2 envelope plasmid (Addgene, cat. no. 12259) and shRNA/pLX302 Luciferase-V5 puro (Addgene, cat. no. 47553), OptiMEM medium (Cellutron life Technologies, cat. no. 31985-070) and Lipofectamine 2000 (Life Technologies, cat. no. 11668-027). HEK293T cells were incubated with the transfection mix first for 4-5 hours, then for 24 hours after addition of DMEM/RPMI medium with 15% and no Abx at 37°C with 5% CO_2. Supernatants were collected and added to the 22RV1 cells directly with 8 μg/mL polybrene in equal amount of antibiotic-free medium. After incubation for 24 hours, cells were split and selected for bioluminescence expression.

In vivo studies

All animal studies were approved and performed according to the Center for Animal Care Procedures (CARE) at Brown University and Institutional Animal Care and Use Committee (IACUC) protocols. Mouse experiments were performed free of pathogens. Four- to five-week old male athymic sp/sp mice were purchased from Taconic and were quarantined in the institution's animal facility for a week before any *in vivo* study was initiated. A total of 2 × 10^6 luciferase expressing 22RV1 (22RV1-LUC) cells were suspended in 100 μl of ice-cold PBS and 100 μl of Matrigel® Basement Membrane Matrix (Corning®, cat. no. 354234). Anesthesia using 100 mg/kg ketamine was performed before a total of 200 μl cell suspension was inoculated subcutaneously into the rear left flank of the mice aged 6-8 weeks. The mice were weighed once a week to monitor signs of drug toxicity. Digital caliper measurements of the length (L), and width (W) of the tumors were taken twice a week to monitor tumor growth. When tumor volume reached an average of 150 mm^3 to 200 mm^3 (calculated using the formula: volume = ½ L × W^2), mice were randomly assigned to control (vehicle) or different treatment groups as indicated in figures.

Vehicle was delivered in 40% PEG400, 5% Tween 80, 5% DMSO and 5% PBS. ONC201 (100 mg/kg, oral gavage, biweekly), enzalutamide (20 mg/kg, oral gavage, daily) and darolutamide (50 mg/kg, oral gavage, twice daily) were delivered in a solution of 40% PEG400, 5% Tween 80, 5% DMSO and 5% PBS. Combination therapy experimental groups are the combination of ONC201 and enzalutamide or the combination of ONC201 and darolutamide. Whole-body bioluminescence imaging using the IVIS Xenogen imaging system was carried out once a week. Mice were intraperitoneally injected with 15 mg/mL D-Luciferin (Goldbio, cat. no. LUCK-1G) and anesthetized with isoflurane. Signal intensities were recorded. The experiment was continued until the tumor burden had reached the ethically allowed limit at 2000 mm^3 in volume or when the mouse had lost more than 20% of its initial body weight. At the end of the experiment, mice were sacrificed per Brown University CARE and IACUC protocols. Tumors and organs were harvested for flow cytometry, immunohistochemistry, serum cytokine profiling using a 42-plex murine cytokine panel for further analysis.

Immunohistochemistry

Tumor and organ tissue sections were used for immunohistochemistry analysis. Resected 22RV1-LUC tumors and other organs from 5 mice each control and treatment groups were fixed in 10% formalin overnight, transferred into 70% ethanol and kept at 4°C before further paraffin treatment. Paraffin embedding, sec-

tioning of slides, and H&E staining were performed by the Pathology Core Facility at Brown University. Sectioned tissue slides were deparaffined using xylene, rehydrated using decreasing concentrations of ethanol and TBS. Heat-induced antigen retrieval was conducted using a vegetable steamer (retrieval buffer: 10 mmol/L of sodium citrate buffer at pH = 6.0) for 20 minutes with temperature maintained at 95°C. After quenching with 3% hydrogen peroxide for 10 minutes and permeabilizing with TBST for 10 minutes, the samples were blocked using 2.5% horse serum (Vector Laboratories), before incubation with primary antibodies overnight at 4°C in a humid chamber. Horseradish peroxidase-conjugated secondary anti-rabbit antibody (Vector Laboratories, ImmPRESS™, HRP-Horse Anti-Rabbit IgG Polymer secondary antibody, cat. no. MP-7401-15) diluted in blocking solution was added to the tissue slides and incubated in humid chamber for 40 minutes at room temperature. The slides were then developed with 3,3'-diaminobenzidine (Vector Laboratories, DAB/Ni Peroxidase Substrate Kit, cat. no. SK-4100) for 5 minutes and counterstained for 4 seconds using hematoxylin. After dehydrating with increasing concentrations of ethanol, the slides were mounted, and a cover slip was added. Images were taken.

Flow cytometry

A total of 2-3 spleens and 2-3 tumors from each short term (1 week) treatment and control groups were processed for flow cytometry analysis. Mouse tumors were processed by finely cutting with razor blades before addition of digestion buffer (75 U/mL Collagenase IV, 125 ug/mL Dispase II, 1% penicillin-streptomycin, in PBS). Tumor pieces were then placed in a 37°C water bath for 30 minutes until fully digested. Digested mouse tumors and spleens were then filtered through a 70 µm cell strainer and washed with PBS. Cells were isolated by centrifugation and resuspended in 2 mL RPMI-1640 medium (HyClone, Cytiva Life Sciences, with 10% FBS and 1% penicillin-streptomycin). 2 mL of 40% or 80% Ficoll-Paque PLUS (Cytiva, cat. no. 17-1440-02, diluted in HBSS with 5% FBS) was added below the cell suspension. Immune cells were further isolated and collected on the interface after centrifugation at 2200 rpm for 30 minutes at room temperature. Processed tumor and spleen immune cells single cell suspensions were then resuspended in 1× Flow Cytometry Staining Buffer (R&D Systems). Staining for membrane surface proteins was conducted using conjugated primary antibody and antibody cocktail for 1 hour on ice. Antibody cocktail added to the samples include anti-CD45 SB600 (eBioscience, cat. no. 63-0451-82, Clone: 30-F11), anti-CD3 molecular complex (17A2) PE (BD Biosciences, cat. no. 555275), anti-CD335 (NKp46) (29A1.4) (Thermo Scientific, cat. no. 17-3351-82, Clone: PK136), anti-CD11b APC/Cy7 (BioLegend, cat. no. 101226, Clone: M1/70), anti-KLRG1 PE/Cy7 (Thermo Scientific, cat. no. 25-5893-82, Clone: 2F1), and anti-CD253 (TRAIL) FITC (Miltenyi Biotec, cat. no. 130-102-447, Clone: N2B2). The controls for each tissue type include unstained control, viability only control stained with Zombie Violet™ (BioLegend, cat. no. 423113), and single stained controls for each antibody used. Cells were then fixed using the EBioscience™ IC Fixation buffer (Thermo Scientific) and incubated in the dark at room temperature for 30 minutes per manufacturer's instructions. 200 µL of Flow Cytometry Staining Buffer (R&D Systems, cat. no. FC001) was added to the cells in 100 µL fixation buffer and filtered into flow cytometry tubes. All samples were kept at 4°C and analyzed via flow cytometry within 48 hours. All data was analyzed using a BD Biosciences LSR II Flow Cytometer and the FlowJo software version 10.8.1 (FlowJo, LLC). Gating strategies are as follows: NK cell: Live/NKp46+/KLRG1+/KLRG1-/TRAIL+/CD11b+.

Cytokine profiling

Murine plasma samples were obtained and analyzed using an R&D Systems Murine Premixed 42plex Multi-Analyte Kit (R&D Systems, Inc.) and a Luminex 200 Instrument (LX200-XPON-RUO, Luminex Corporation) in accordance with the manufacturer's instructions. Samples were analyzed for levels of GM-CSF, CXCL1/GRO alpha/KC/CINC-1, IL-7, GDF-15, CCL2/JE/MCP-1, IL-1 beta/IL-1F2, Chitinase-3-Like 1, VEGF, IL-2, IL-4, VEGFR2/KDR/Flk-1, IL-6, IL-10, IL-17/IL-17A, IFN-gamma, IL-3, IL-16, CXCL10/IP-10/CRG-2, CCL5/RANTES, CCL7/MCP-3/MARC, CCL12/MCP-5, IL-33, Prolactin, M-CSF, CCL3/MIP-1alpha, IL-1 alpha/IL-1F1, CCL20/MIP-3alpha, TWEAK/TNFSF12, CXCL12/SDF-1 alpha, IGF-1, IL-27, BAFF/Blys/TNFSF13B, MMP-8, MMP-3, Granzyme B, Angiopoietin-2, CCL21/6Ckine, MMP-12, CCL12/

Table 1. Prostate cancer cell lines used in the study

Cell Lines	Source of origin	AR status	Known key mutations	Castration sensitivity	Source	Reference
22RV1	Primary xenograft	+	BRCA2 deficient, AR-V7 positive	Resistant	ATCC	[35]
LNCaP	Lymph node metastasis	+	DDR deficient	Sensitive	ATCC	[36]
DU145	Brain metastasis	-	BRCA (non-pathogenic)	Resistant	ATCC	[37]
PC3	Bone metastasis	-	PTEN deletion (homozygous)	Resistant	ATCC	[38]

Eotaxin, CCL22/MDC, and Dkk-1, values were reported in pg/mL.

Statistical analysis

For *in vitro* studies, all statistical analyses and graph generations were conducted using GraphPad Prism version 9.3.0. Data are presented as mean ± SD from at least three replicates for each experiment. The statistical significance comparing two groups was determined using the Student's t-test. A minimal level of significance was set to be $P < 0.05$ (*$P < 0.05$, **$P < 0.01$, ***$P < 0.001$). For *in vivo* studies, all statistical analysis and graph generations were conducted using GraphPad Prism version 9.3.0. Data are presented as mean ± SD from at least three technical replicates for each experiment. The statistical differences between treatment groups and controls were determined using one-way ANOVA test with a minimal level of significance of $P < 0.05$ (*$P < 0.05$, **$P < 0.01$, ***$P < 0.001$).

Results

Darolutamide reduces viability of prostate cancer cell lines as single agent

It has been previously shown that darolutamide does not activate mutant AR such as AR (W742L), AR (T878A) and AR (F877L), and has a low inhibition constant (Ki) and maximal inhibitory concentration (IC50) when tested in AR-HEK293 cells stably expressing full-length AR [26]. When compared to other next-generation non-steroidal antiandrogens such as enzalutamide or apalutamide, darolutamide has a negligible blood-brain-barrier penetration, which may contribute to an improved CNS adverse effect (AE) [27]. To evaluate the *in vitro* efficacy of darolutamide against castration-resistant prostate cancer, 22RV1, LNCaP, PC3, and DU145 prostate cancer cell lines with distinct properties were treated with different concentrations of darolutamide in a CellTiter-Glo cell viability assay (**Table 1**).

The half-maximal inhibitory concentration (IC50) was calculated for each cell line from the dose-response curves (**Figure 1**) to measure the potency of darolutamide in inhibiting cell proliferation. All four cell lines displayed high sensitivity to darolutamide, with an IC50 of 46.6 μM for 22RV1, 33.8 μM for LNCaP, 32.3 μM for PC3 and 11.0 μM for DU145. Increased ATF4 expression was observed in darolutamide-treated 22RV1 and LNCaP cells and reduced prostate specific antigen (PSA) was observed in LNCaP cells (**Figures 2**, **3**). Although co-treatment with DHT rescued some effects of darolutamide in reducing PSA and induction of ATF4, darolutamide showed better PSA reduction in LNCaP cells and ATF4 induction in both LNCaP and compared to cells treated with enzalutamide (**Figure 3**). Interestingly, darolutamide demonstrated higher inhibition potency in metastatic prostate cancer PC3 and DU145 cell lines, despite their androgen independence. Western blot analysis suggested that darolutamide may activate other pathways to reduce AR activity. In summary, darolutamide alone can upregulate the integrated stress response and reduce PSA levels in castration-resistant or castration-sensitive prostate cancer cells *in vitro.*

ONC201 synergizes with enzalutamide or darolutamide against prostate cancer cells in vitro

We previously reported that ONC201 has anti-proliferative and pro-apoptotic effects in various prostate cancer cell lines by upregulation of TRAIL, DR5 and induction of the integrated stress response (ISR) through ATF4 [24]. With the observation that darolutamide is effective in treating prostate cancer as a single agent, its potential benefits in combination with ONC201 were further evaluated here. For comparison, combination of ONC201 with enzalutamide was included in the study. The IC50 of ONC201, enzalutamide or darolutamide were calculated

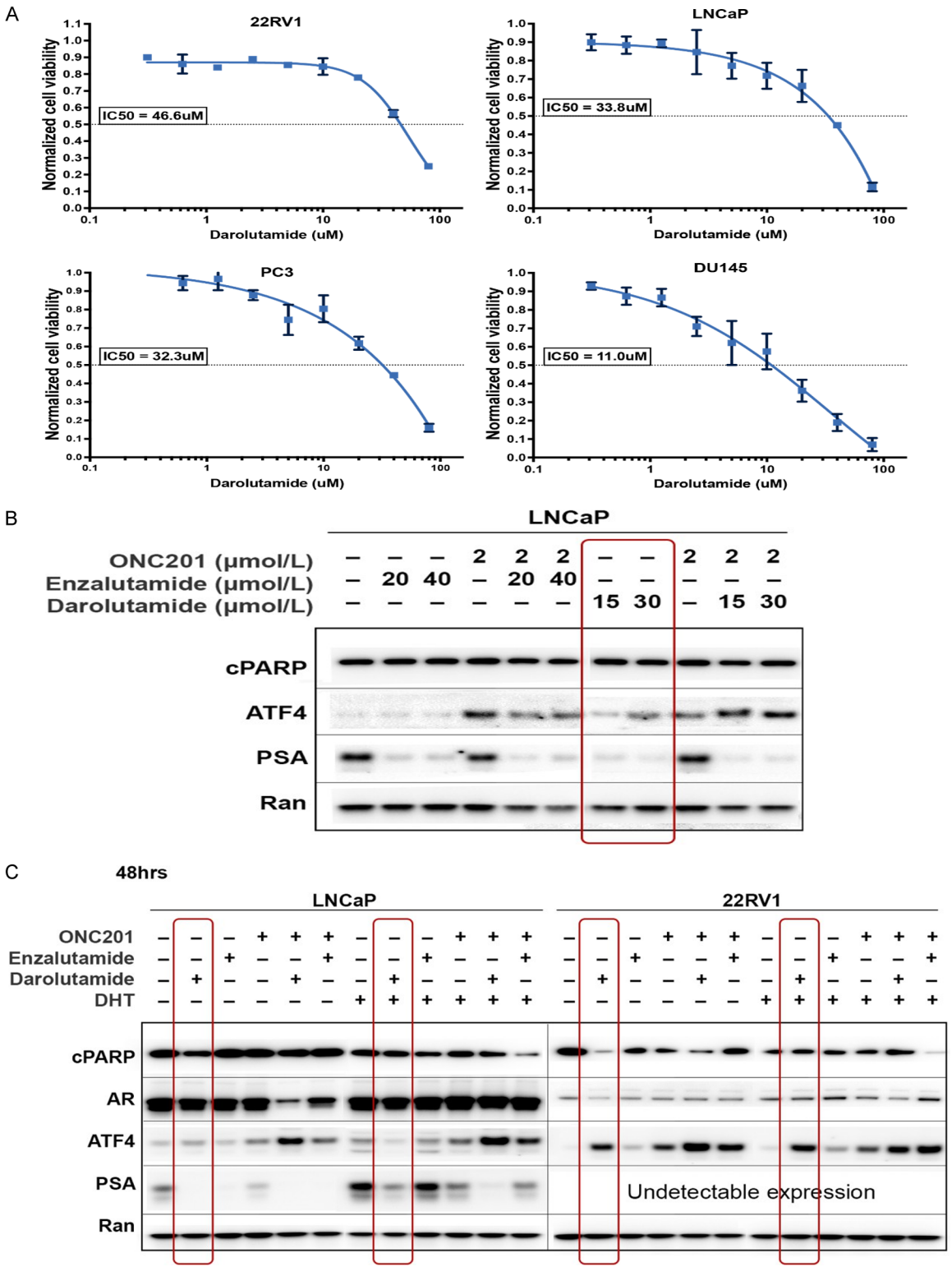

Figure 1. Dose-response curves and IC50s for darolutamide and effects on PSA, ATF4 in prostate cancer cell lines. A. Proapoptotic and antiproliferation effects were measured using the CTG assay in 22RV1, LNCaP, PC3 and DU145 cell lines at 72 hours post treatment. Representative dose-response curves and calculated IC50s for darolutamide in each cell line are shown. B. Darolutamide reduces PSA and induces ATF4 in the LNCaP cell line. Western blot analysis of the LNCaP cell line treated with ONC201, enzalutamide or darolutamide as single agents or in combinations are shown. The red box highlights the single agent effect of darolutamide on ATF4 and PSA. C. Darolutamide reduces

PSA and induces ATF4 in LNCaP and 22RV1 cell lines regardless of DHT activation. AR signaling was stimulated by addition of 1 μg/mL DHT. AR-expressing LNCaP and 22RV1 cell lines were co-treated with ONC201, enzalutamide or darolutamide as single agents or in combinations. The red boxes highlight the single agent effect of darolutamide on AR, ATF4, or PSA in the presence and absence of DHT in the LNCaP or 22RV1 cell lines as indicated.

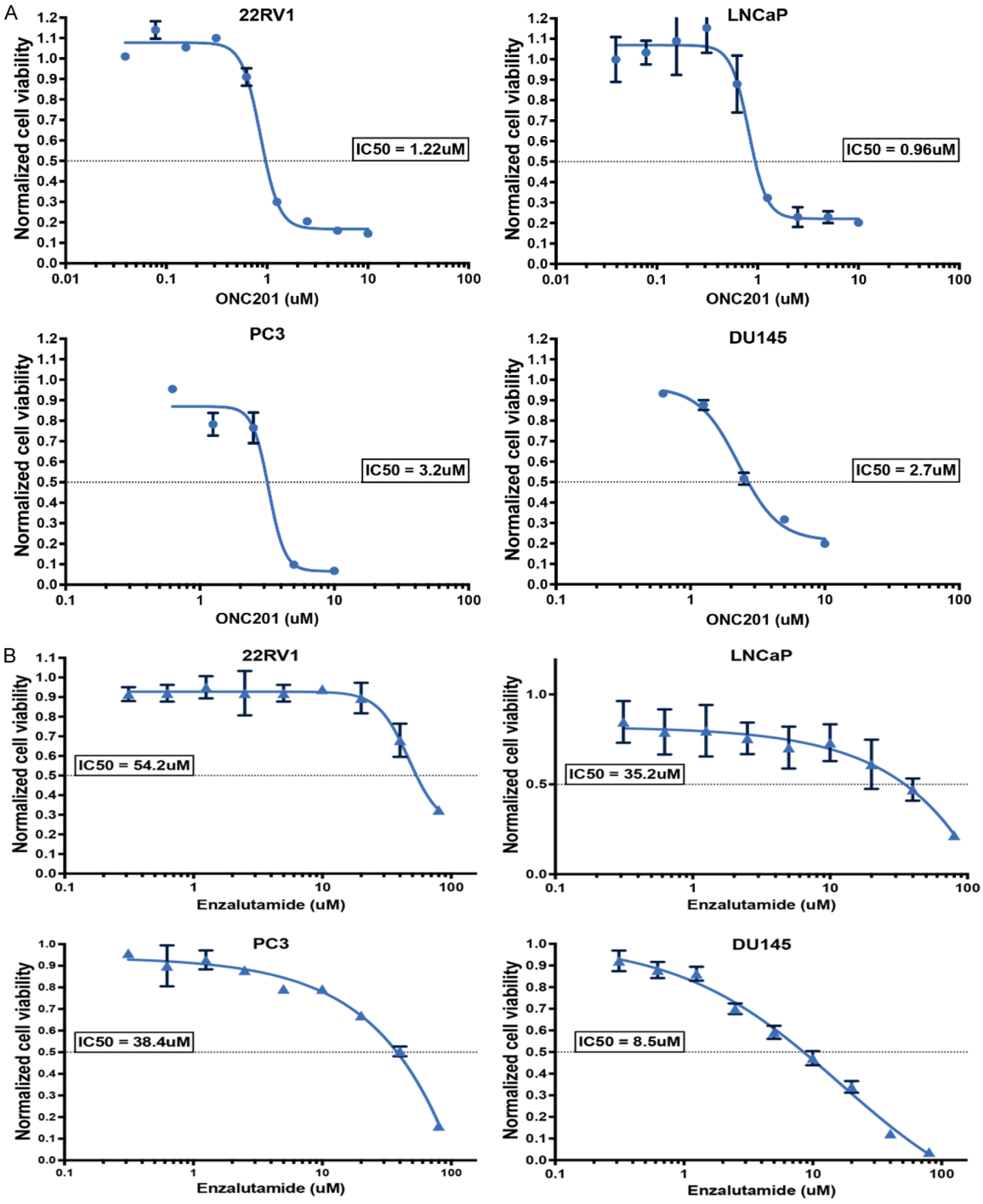

Figure 2. Representative dose-response curves and IC50 values for ONC201 and enzalutamide in four prostate cancer cell lines. A. Proapoptotic and antiproliferation effects were assessed using the CTG cell viability assay in the 22RV1, LNCaP, PC3 or DU145 human prostate cancer cell lines at 72 hours post drug treatment. Dose-response curves and calculated IC50s for ONC201 in each cell line are shown. B. Proapoptotic and antiproliferation effects were measured using the CTG cell viability assay in the 22RV1, LNCaP, PC3 and DU145 human prostate cancer cell lines at 72 hours post-treatment. Representative dose-response curves and calculated IC50s of enzalutamide for each cell line are shown.

A

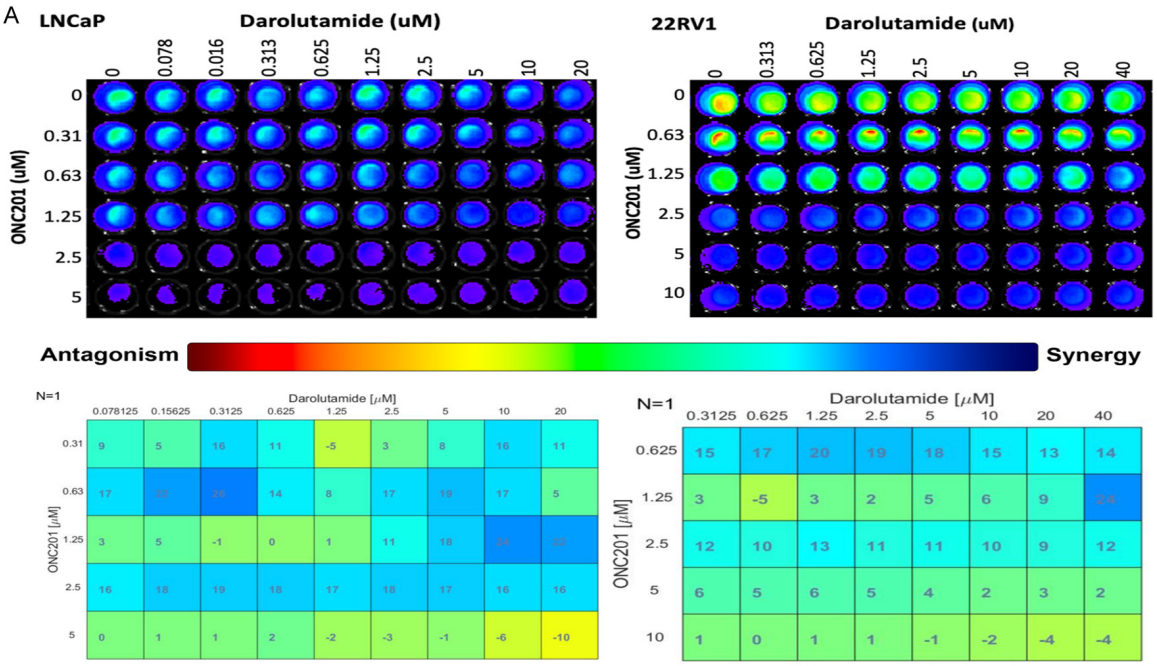

B

LNCaP		Darolutamide (uM)								
		0.078	0.156	0.313	0.625	1.25	2.5	5	10	20
ONC201 (uM)	0.3125	0.64	2.31	0.29	0.32	1.84	0.46	0.27	0.19	0.20
	0.625	0.63	0.51	0.43	0.57	0.66	0.44	0.38	0.37	0.50
	1.25	1.06	0.99	1.21	1.17	1.13	0.80	0.67	0.56	0.58
	2.5	0.56	0.51	0.49	0.51	0.53	0.51	0.53	0.56	0.56
	5	0.80	0.80	0.75	0.75	0.93	0.98	0.89	1.12	1.26

22RV1		Darolutamide (uM)							
		0.3125	0.625	1.25	2.5	5	10	20	40
ONC201 (uM)	0.625	0.75	0.65	0.59	0.62	0.63	0.63	0.65	0.54
	1.25	0.92	1.30	0.91	0.95	0.84	0.81	0.71	0.38
	2.5	0.43	0.48	0.38	0.45	0.43	0.47	0.47	0.43
	5	0.56	0.60	0.56	0.60	0.64	0.68	0.68	0.72
	10	1.12	1.20	1.11	1.19	1.27	1.35	1.52	1.52

Figure 3. ONC201 synergizes with darolutamide against LNCaP and 22RV1 human prostate cancer cell lines *in vitro*. A. Combinations of ONC201 (0-5 μM or 10 μM) and darolutamide (0-20 μM or 40 μM) were evaluated in LNCaP and 22RV1 human prostate cancer cell lines at 72 hours post treatment using the CTG cell viability assay. Synergistic doses are shown. B. Representative CI indices for combination of ONC201 and darolutamide in LNCaP and 22RV1 cell lines are shown. Highlights in yellow indicate synergy.

from dose-response curves using CTG cell viability assay for single drugs and for each of indicated combination therapy groups in LNCaP, 22RV1, PC3 and DU145 cells (**Figure 2**).

Combination indices (CI) and heat maps showing synergy and antagonism in the ONC201 and enzalutamide or darolutamide groups for all four prostate cancer cell lines were generated (**Figures 3**-**6**).

The androgen receptor (AR) signaling pathway is overactive in advanced forms of prostate cancer, altering expression of genes that contribute to uncontrolled cell proliferation and cancer survival [28]. Despite being hormone dependent, most forms of castration-resistant prostate cancer (CRPC) rely on AR and AR-dependent signaling pathways and this eventually leads to antiandrogen therapy resistance [29]. Therefore, we hypothesized that by combining ONC201 and androgen receptor signaling antagonists, enzalutamide or darolutamide, the anti-proliferative and pro-apoptotic properties of ONC201 may be increased and that this may subsequently enhance inhibitory effects of

A

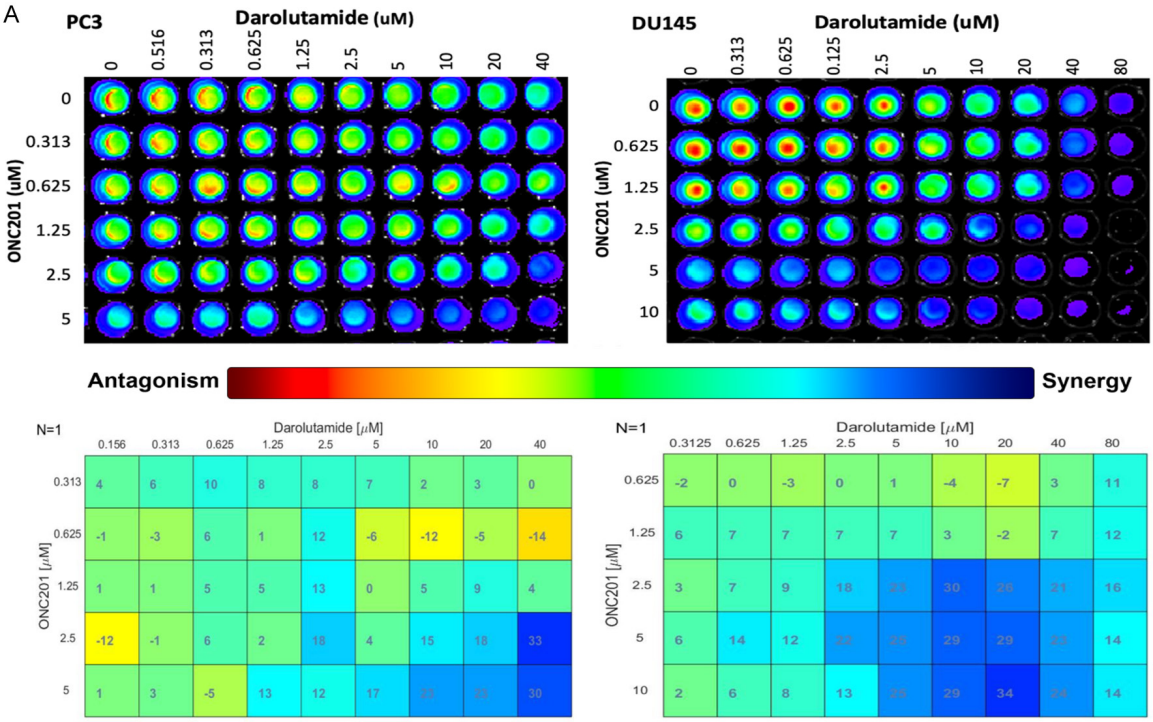

B

PC3		Darolutamide (uM)								
		0.15625	**0.3125**	**0.625**	**1.25**	**2.5**	**5**	**10**	**20**	**40**
ONC201 (uM)	**0.3125**	0.74	0.51	0.35	0.47	0.50	0.66	1.04	1.11	1.65
	0.625	3.11	22.83	0.88	1.53	0.56	2.84	4.27	1.92	3.75
	1.25	1.37	1.45	1.02	1.19	0.78	1.86	1.18	1.02	1.54
	2.5	2.41	1.12	0.80	1.04	0.54	1.16	0.86	0.89	0.45
	5	0.69	0.66	0.89	0.44	0.49	0.42	0.35	0.43	0.38

DU145		Darolutamide (uM)								
		0.313	**0.625**	**1.25**	**2.5**	**5**	**10**	**20**	**40**	**80**
ONC201 (uM)	**0.313**	3.65	1.66	2.33	1.33	1.26	1.51	1.65	0.99	0.45
	0.625	0.99	0.99	1.03	1.05	1.03	1.21	1.43	0.86	0.41
	1.25	0.63	0.60	0.64	0.57	0.63	0.50	0.43	0.37	0.23
	2.5	0.69	0.57	0.63	0.50	0.51	0.51	0.52	0.40	0.41
	5	1.46	1.32	1.29	1.18	0.88	0.83	0.60	0.52	0.54

Figure 4. ONC201 synergizes with darolutamide against PC3 and DU145 human prostate cancer cell lines *in vitro.* (A) Combinations of ONC201 (0-5 μM or 10 μM) and darolutamide (0-40 μM or 80 μM) were evaluated in PC3 and DU145 human prostate cancer cell lines at 72 hours post treatment using the CTG cell viability assay. Synergistic doses are shown. (B) Representative CI indices for combination of ONC201 and darolutamide in PC3 and DU145 cell lines are shown. Highlights in yellow indicate synergy. The 10 μM ONC201 analysis is missing for DU145 cells in the CI analysis but is shown in (A) both in the primary data and synergy analysis.

enzalutamide or darolutamide against AR. Indeed, the heat map results reveal that ONC201 synergizes with darolutamide (**Figures 3A**, **4A**), or enzalutamide in all of the four cell lines (**Figures 5A**, **6A**), with the most synergistic combination doses shown in in dark blue. Heat maps of CIs for each drug combination also yielded consistent results showing best synergistic doses with combination indices lower than 0.5 as highlighted in yellow (**Figures 3B**, **4B**, **5B**, **6B**).

The cell viability assay results showed that all four of the prostate cancer cell lines tested were sensitive to combinations of ONC201 and enzalutamide or darolutamide at multiple specific drug concentrations. Strong synergy from the combination of ONC201 and darolutamide

A

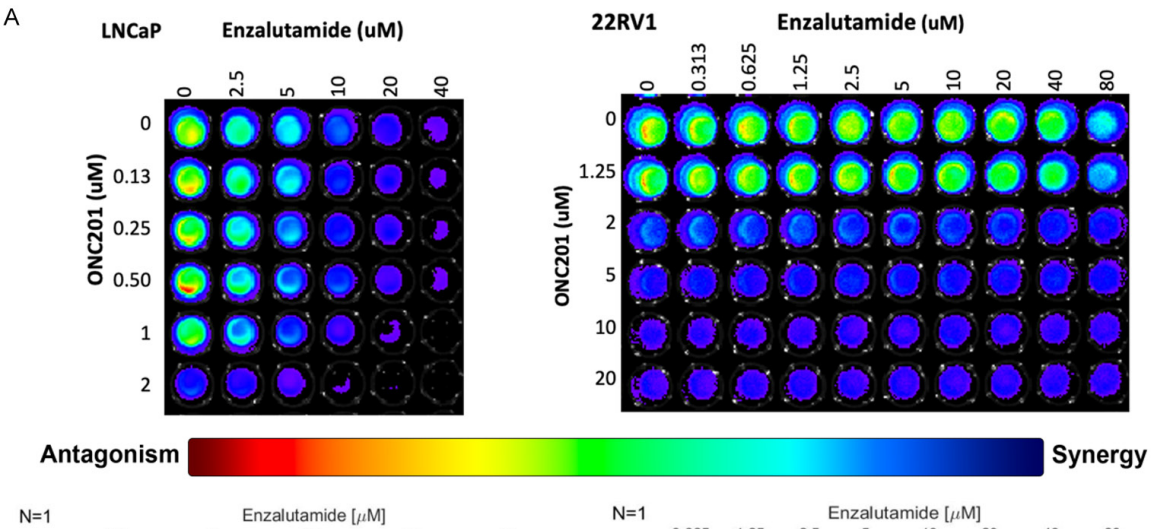

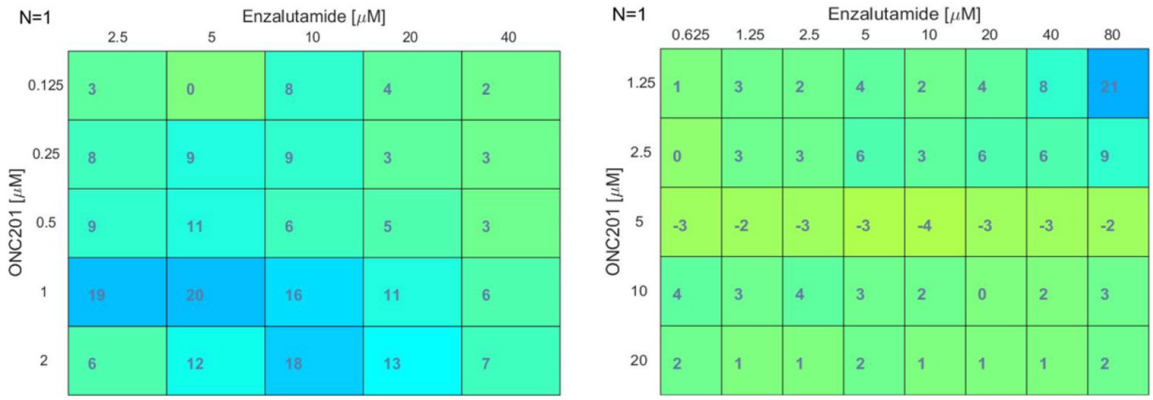

B

LNCaP		Enzalutamide (uM)				
		2.5	5	10	20	40
ONC201 (uM)	0.13	0.21	1.10	0.73	0.87	0.87
	0.25	0.93	0.86	0.78	0.97	0.87
	0.5	1.11	0.93	0.97	0.91	0.94
	1	1.15	0.89	0.75	0.62	0.60
	2	0.82	0.67	0.55	0.65	0.65

22RV1		Enzalutamide (uM)							
		0.625	1.25	2.5	5.0	10.0	20.0	40.0	80.0
ONC201 (uM)	1.25	1.13	0.85	0.94	0.76	0.83	0.65	0.52	0.35
	2.5	0.33	0.31	0.31	0.28	0.30	0.28	0.28	0.25
	5	0.47	0.45	0.45	0.47	0.47	0.47	0.47	0.45
	10	0.71	0.71	0.68	0.71	0.75	0.81	0.78	0.71
	20	1.49	1.56	1.56	1.49	1.56	1.56	1.56	1.49

Figure 5. ONC201 synergizes with enzalutamide against LNCaP and 22RV1 human prostate cancer cell lines *in vitro*. A. Combinations of ONC201 (0-2 μM or 20 μM) and enzalutamide (0-40 μM or 80 μM) were evaluated in LNCaP or 22RV1 human prostate cancer cell lines at 72 hours post treatment using the CTG cell viability assay. Synergistic doses are shown. B. Representative CI indices for combination of ONC201 and enzalutamide in LNCaP and 22RV1 cell lines are shown. Highlights in yellow indicate synergy.

was observed across all four cell lines, whether metastatic (PC3, DU145, LNCaP) or non-metastatic (22RV1), castration resistant (22RV1, PC3, DU145) or sensitive (LNCaP), AR-positive

A

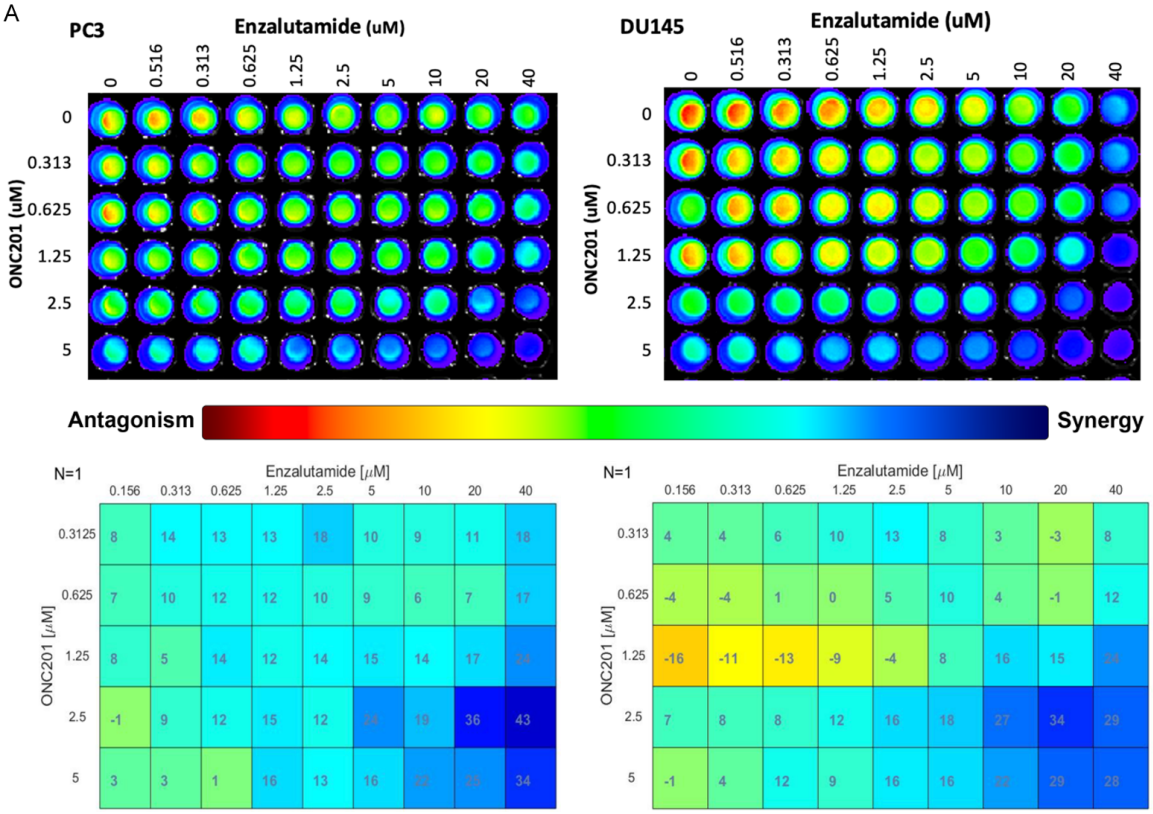

B

PC3		Enzalutamide (uM)								
		0.15625	0.3125	0.625	1.25	2.5	5	10	20	40
ONC201 (uM)	0.3125	0.30	0.19	0.22	0.24	0.23	0.45	0.66	0.85	0.89
	0.625	0.57	0.44	0.40	0.41	0.49	0.63	0.91	1.21	0.99
	1.25	0.65	0.80	0.52	0.61	0.65	0.64	0.78	0.85	0.82
	2.5	1.00	0.67	0.61	0.56	0.67	0.49	0.69	0.45	0.42
	5	0.73	0.74	0.79	0.48	0.55	0.51	0.43	0.43	0.32

DU145		Enzalutamide (uM)								
		0.15625	0.3125	0.625	1.25	2.5	5	10	20	40
ONC201 (uM)	0.3125	0.60	0.70	0.65	0.63	0.70	1.11	1.15	1.08	0.35
	0.625	1.36	1.45	0.98	1.33	1.10	1.10	1.30	1.06	0.29
	1.25	2.95	1.93	2.39	1.93	1.58	0.96	0.82	0.54	0.13
	2.5	0.67	0.65	0.65	0.56	0.50	0.49	0.37	0.25	0.11
	5	0.96	0.78	0.54	0.64	0.47	0.49	0.36	0.25	0.19

Figure 6. ONC201 synergizes with enzalutamide against PC3 and DU145 human prostate cancer cell lines *in vitro*. A. Combinations of ONC201 (0-5 μM) and enzalutamide (0-40 μM) were evaluated in PC3 or DU145 human prostate cancer cell lines at 72 hours post treatment using the CTG cell viability assay. Synergistic doses are shown. B. Representative CI indices for combination of ONC201 and enzalutamide in PC3 and DU145 cell lines are shown. Highlights in yellow indicate synergy.

(22RV1, LNCaP) or AR-negative (PC3, DU145) (**Figures 3**, **4**). Darolutamide showed synergy with ONC201 at lower doses as compared to enzalutamide. This is consistent with previously reported preclinical results with darolutamide, including having higher AR-inhibitory potency and an ability to bypass activation of mutant AR, unlike other antiandrogens such as enzalutamide or apalutamide [26]. The AR3 (AR-V7), a constitutively active AR-variant whose transcriptional activity is independent of androgen or anti-androgen activity, has shown resistance

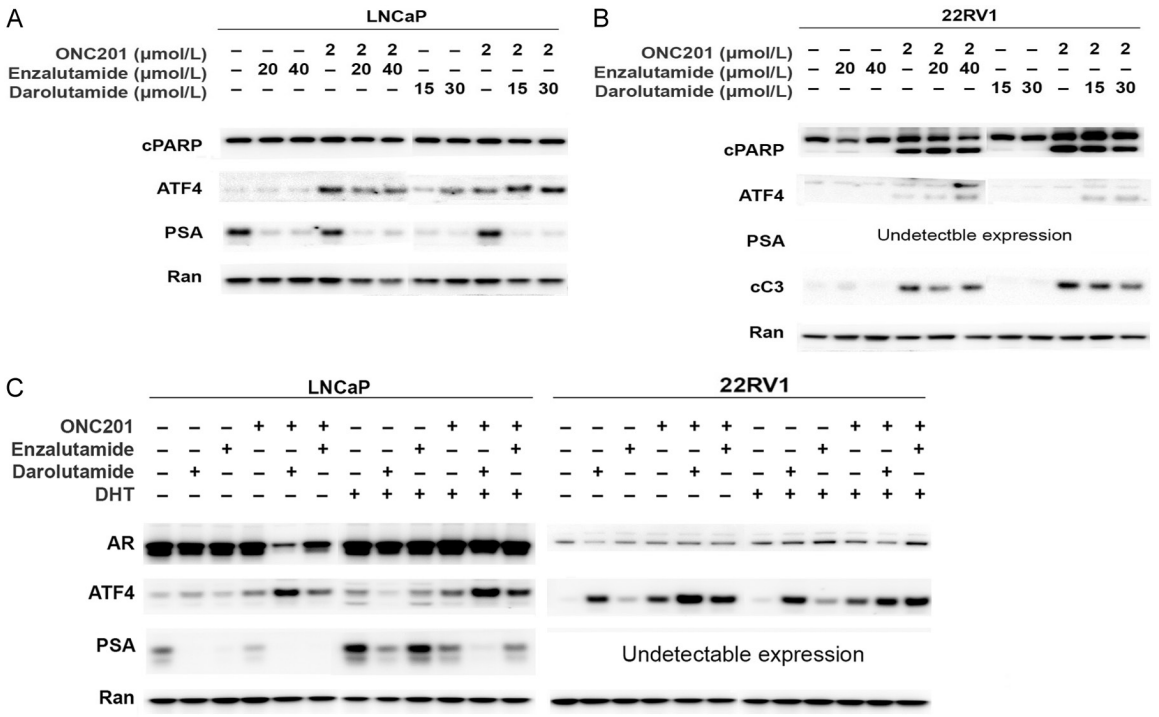

Figure 7. Effects of combinations of ONC201 with darolutamide or enzalutamide on PSA, ATF4, and PARP cleavage in human prostate cancer cell lines. A. Western blot analysis of LNCaP cells treated with 2 μM of ONC201, enzalutamide (20 μM or 40 μM) or darolutamide (15 μM or 30 μM) as single agents or in combinations for 48 hours as compared with control untreated cells. This is the same as **Figure 1B** reproduced here for convenience. B. Western blot analysis of 22RV1 cells treated with 2 μM of ONC201, enzalutamide (20 μM or 40 μM) or darolutamide (15 μM or 30 μM) as single agents or in combinations for 48 hours as compared with control untreated cells. C. AR signaling was induced by DHT (1 μg/mL) treatment in AR-expressing LNCaP and 22RV1 cell lines. Western blot analysis of LNCaP and 22RV1 cells treated with 2 μM ONC201, 40 μM enzalutamide or 30 μM darolutamide as single agents or in combinations for 48 hours is shown as compared with control untreated cells.

against existing androgen receptor antagonists such as enzalutamide and apalutamide which may have contributed to less synergy from combination of ONC201 with enzalutamide in AR-V7 positive 22RV1 cells. Overall, the *in vitro* drug combination results show improved anti-tumor efficacy with ONC201 and darolutamide or enzalutamide in treating both non-metastatic and metastatic prostate cancer cells in culture.

Combination of ONC201 with darolutamide reduces PSA level, activates ISR and promotes apoptosis in prostate cancer cell lines

To further evaluate and compare anti-tumor efficacy among treatment groups with enzalutamide or darolutamide, LNCaP and 22RV1 cells were treated with ONC201, darolutamide or enzalutamide as single agents or in combinations for 48 hours for protein marker analysis. The pro-apoptotic and anti-proliferative characteristics of ONC201 were confirmed in western blot analysis in the 22RV1 cell line (**Figure 7A**, **7B**).

It has been previously reported that ATF3, a stress response mediator downstream of ATF4 is a repressor of AR and is upregulated by ONC201, and that the induction of both ATF4 and ATF3 is associated with reduction of PSA levels [24]. Western blot results at 48 hours showed upregulation of ATF4 when cells were treated with ONC201, enzalutamide and darolutamide alone. Upregulation of ATF4 was observed in ONC201 and darolutamide combination groups where higher doses of darolutamide yielded more ATF4 activation (**Figure 7A**, **7B**). Though less ATF4 induction was seen in the 22RV1 cell line, similar results were observed as ISR was induced in response to combinations of ONC201 and enzalutamide or darolutamide. PSA level was significantly reduced by enzalutamide or darolutamide alone or in combinations with ONC201 in LNCaP cells. Of note, ONC201 treatment alone

showed less reduction in PSA level compared to darolutamide, enzalutamide and combinations, and ATF4 induction had no correlation with PSA levels in LNCaP cells.

Since darolutamide and enzalutamide demonstrated efficacies in reducing PSA levels, and combinations with ONC201 showed increased induction in ATF4, the effect of a more potent androgen receptor ligand, dihydrotestosterone (DHT), in activating AR and treatment efficacies was evaluated (**Figure 7C**). DHT (1 μg/mL) was co-administered with ONC201, enzalutamide, darolutamide or their indicated combinations. Western blot analysis revealed that darolutamide and enzalutamide alone reduced PSA level and induced ATF4 in both LNCaP and 22RV1 cell lines regardless of the presence or absence of DHT (**Figure 7C**). The combination of ONC201 and darolutamide also showed increased induction of AR in both tested cell lines as compared to combination of ONC201 and enzalutamide. In lane 5 of **Figure 7C**, combination of ONC201 with darolutamide significantly reduced AR expression, upregulated ATF4 and reduced PSA in LNCaP cells. Although not as significant, in lane 11 of the same figure with addition of DHT, the ONC201 and darolutamide combination had the same antiproliferative, pro-apoptotic and AR inhibitory effects. Of note, DHT treatment did not increase AR expression in 22RV1 (**Figure 7C**). This is consistent with previous reports suggesting that DHT is unable to stimulate the transcription as the AR isoforms in 22RV1 cells lack the COOH-terminal hormone binding domain (ARΔCTD) [30].

Taken together, the anti-proliferative and pro-apoptotic properties of ONC201 synergized with darolutamide, an anti-androgen receptor signaling agent with a higher AR signaling inhibition potency as compared to enzalutamide. The cell culture results shed light on the potential benefits of a novel combination therapy using ONC201 and darolutamide against CRPC. The results also support further evaluation of the anti-tumor efficacy, toxicity, and therapeutic benefits of the ONC201 plus enzalutamide or darolutamide drug combination *in vivo.*

Treatment-induced TRAIL activation within NK cells in a 22RV1 prostate cancer xenograft model

Since combinations of ONC201 with enzalutamide or darolutamide were synergistic *in vitro,* both combinations were further investigated *in vivo* using a subcutaneously inoculated 22RV1-LUC xenograft model with immunodeficient male mice. Mice were randomly assigned to vehicle treated control groups or experimental groups and treated with 100 mg/kg ONC201 (oral gavage, twice a week), 20 mg/kg enzalutamide (oral gavage, daily), or 50 mg/kg darolutamide (oral gavage, twice daily) as single agents or combinations of ONC201 and enzalutamide or darolutamide. Tumor volumes were measured using a digital caliper twice a week. Mice were further divided into short term (1 week, n = 2 or 3 per group) and long term (6 weeks, n = 6 or 7 per group) treatment groups.

Immune modulation was evaluated in the short-term (1 week) treatment groups via flow cytometric analysis. Levels of spawning/homing (**Figure 8A**) and intra-tumoral/migrating (**Figure 8B**) KLRG1-, TRAIL+, and CD11b+ NK cells were measured to determine stages of the NK cells, TRAIL activation, and NK cell maturation, respectively. Although no significance was shown due to sample size and the short-term treatment time-line, trends of intra-tumoral NK cells were observed (**Figure 8B**), as represented by the NKp46+ cells. Overall trends of increasing TRAIL induction by the anti-androgen and combination groups with ONC201 were also present in the tumors (**Figure 8B**). Integrin CD11b is used as an NK cell maturation marker in mice, with CD11b+ NK cells indicating maturation. In **Figure 8B**, trends of migrating NK cells were observed in the tumors of the mice. NK cell maturation indicated by increasing levels of CD11b+ cells suggest a treatment-induced immune response, which may contribute to eventual partial tumor regression.

Treatment-induced immune modulation may contribute to partial tumor regression in the 22RV1 prostate cancer xenograft model

To further understand the immune effects of drug treatments, whole blood was collected from mice (n = 9 for partial responders, n = 21 for non-responders) upon sacrifice and purified serum was analyzed for expression of a panel of murine cytokines (**Figure 9A**). The overall results were largely heterogenous across all cytokines when comparing single treatments, combinations, and control groups (**Figure 9A**). However, after regrouping as partial responders (mice that showed signs of tumor regression) and non-responders (mice that did not show signs of tumor regression), a comparison

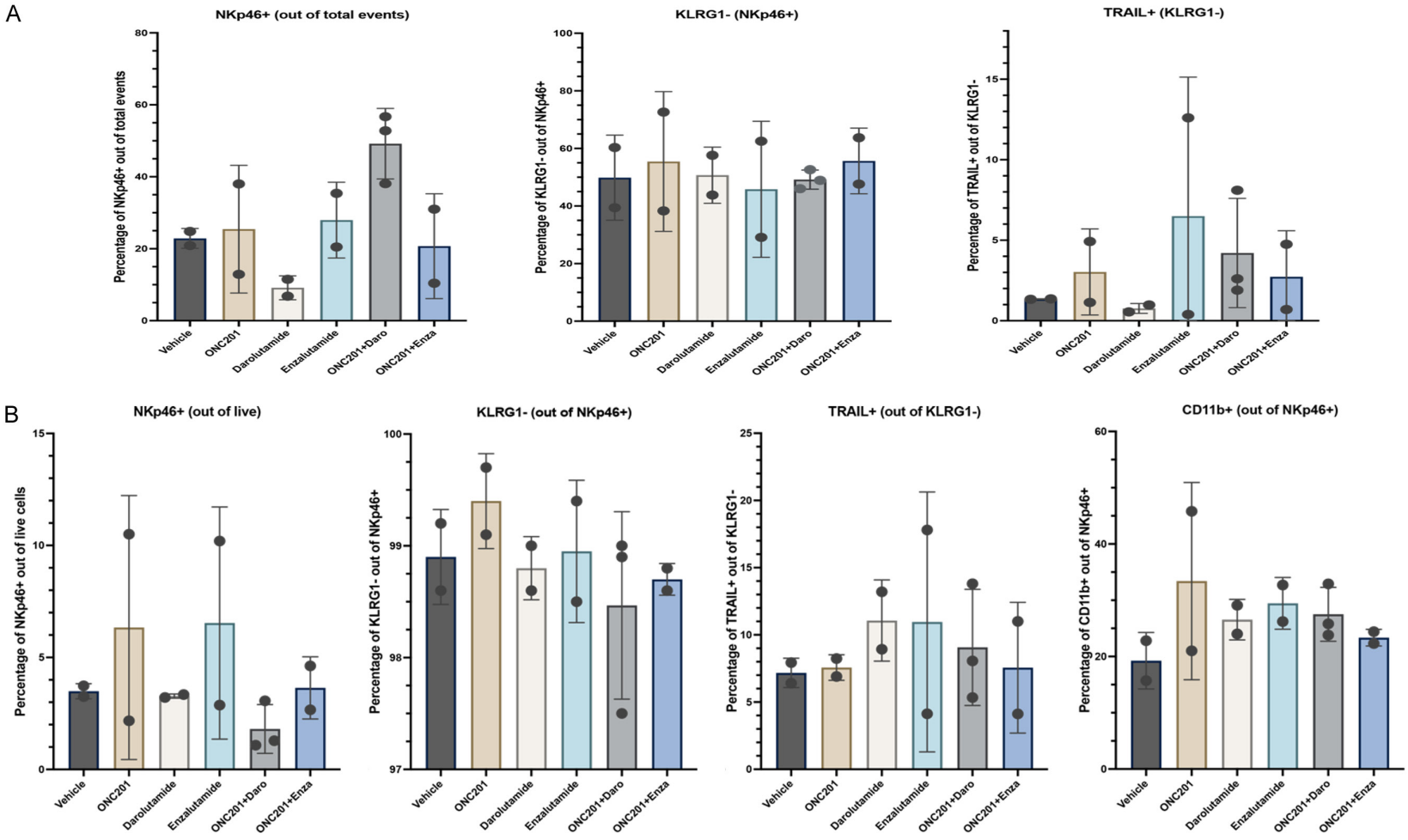

Figure 8. Mouse spleen and tumor flow cytometry results showing trends of TRAIL activation within NK cells. A. Graphs summarizing flow cytometry data for KLRG1- and TRAIL+ NK cells in spleens of mice in the control and treatment groups at 7 days post treatment. Results represent mean ± SEM of one experiment, showing trends indicating circulating NK cells and TRAIL activation in treatment groups (n = 2 for all experimental and control groups except for group treated with combinations of ONC201 and darolutamide where n = 3). B. Graphs summarizing flow cytometry data for KLRG- TRAIL+ CD11b+ NK cells in 22RV1-LUC subcutaneous tumors of mice in indicated control and treatment groups at 7 days post treatment. Results presented as mean ± SD of one experiment with 2 to 3 mice per group, showing trends indicating infiltrating NK cells and TRAIL activation in treatment groups.

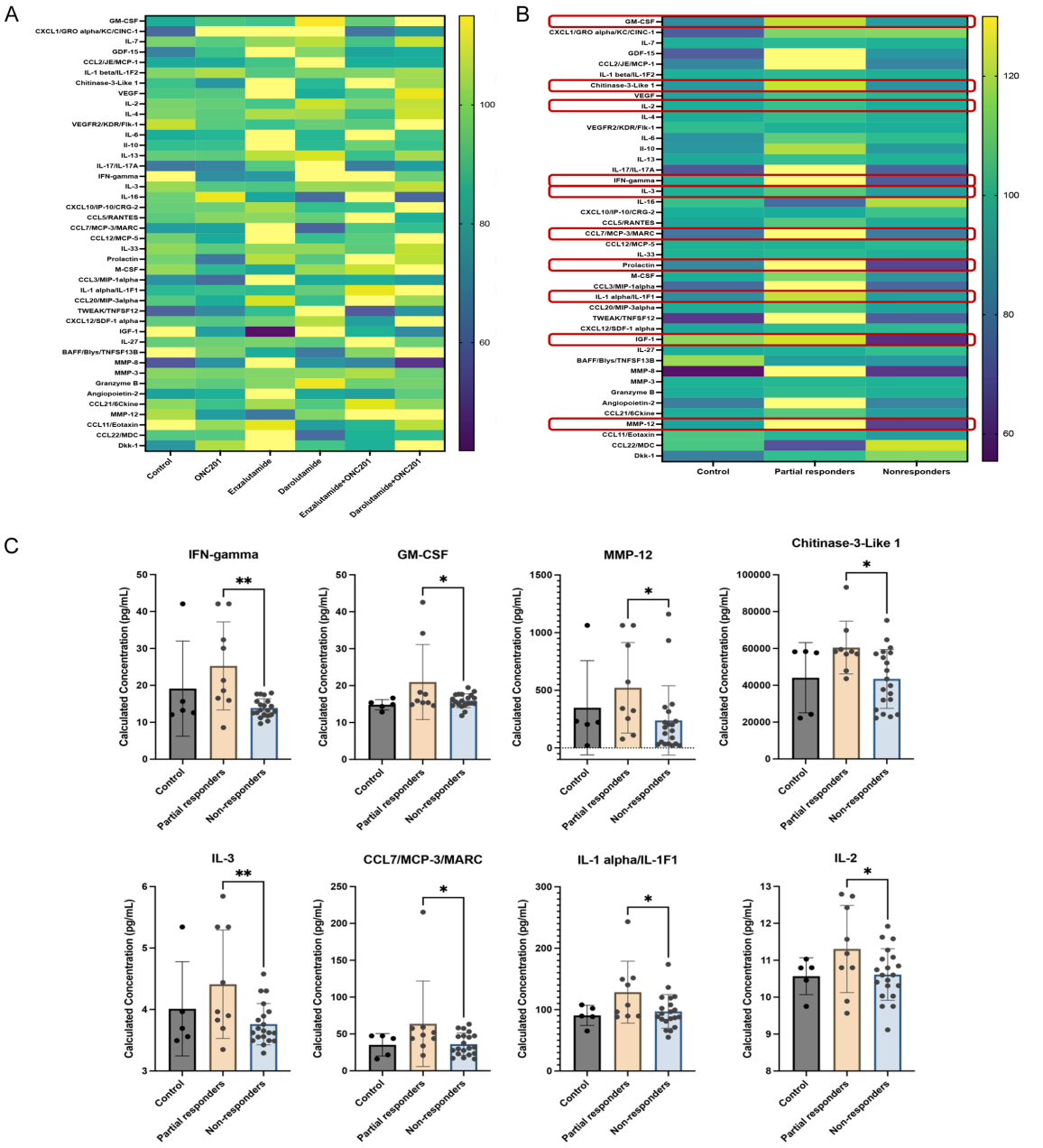
A
GM-CSF
CXCL1/GRO alpha/KC/CINC-1
IL-7
GDF-15
CCL2/JE/MCP-1
IL-1 beta/IL-1F2
Chitinase-3-Like 1
VEGF
IL-2
IL-4
VEGFR2/KDR/Flk-1
IL-6
Il-10
IL-13
IL-17/IL-17A
IFN-gamma
IL-3
IL-16
CXCL10/IP-10/CRG-2
CCL5/RANTES
CCL7/MCP-3/MARC
CCL12/MCP-5
IL-33
Prolactin
M-CSF
CCL3/MIP-1alpha
IL-1 alpha/IL-1F1
CCL20/MIP-3alpha
TWEAK/TNFSF12
CXCL12/SDF-1 alpha
IGF-1
IL-27
BAFF/Blys/TNFSF13B
MMP-8
MMP-3
Granzyme B
Angiopoietin-2
CCL21/6Ckine
MMP-12
CCL11/Eotaxin
CCL22/MDC
Dkk-1
100
80
60
Control
ONC201
Enzalutamide
Darolutamide
Enzalutamide+ONC201
Darolutamide+ONC201
B
120
100
80
60
Control
Partial responders
Nonresponders
C
IFN-gamma
GM-CSF
MMP-12
Chitinase-3-Like 1
IL-3
CCL7/MCP-3/MARC
IL-1 alpha/IL-1F1
IL-2
Calculated Concentration (pg/mL)
Control
Partial responders
Non-responders
D a
ONC201 vs. Control
BAFF/Blys/TNFSF13B
CXCL/GRO alpha/
KC/CINC-1
IGF-1
-log10 (p value)
log2(Fold Change)
b
Enzalutamide vs. Control
BAFF/Blys/TNFSF13B
VEGF
IGF-1
IL-6
GDF-15
CCL7/MCP-3/MARC
CCL3/
MIP-1 alpha
-log10 (p value)
log2(Fold Change)

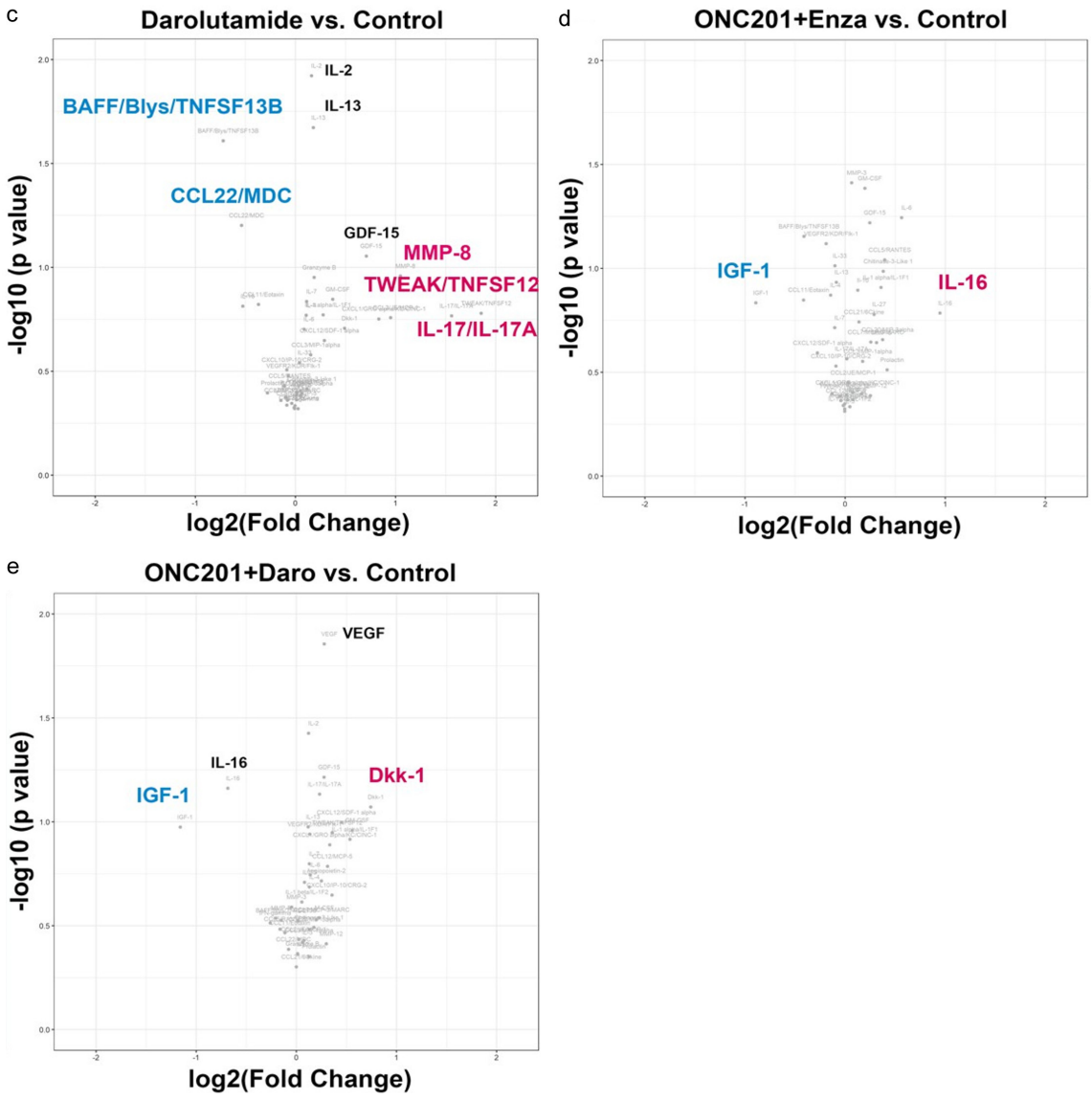

Figure 9. Cytokine profiling of serum in 22RV1 tumor-bearing mice treated with ONC201, enzalutamide, darolutamide, or combinations as indicated. A. Heat map of cytokine expression levels for mice in control (vehicle) group or experimental groups treated with ONC201, enzalutamide, darolutamide or indicated combinations. The row maximum is shown in full yellow and row minimum is shown in full dark purple. B. Heat map of relative cytokine expression levels for mice that showed partial tumor regression (partial-responders) and those that did not show any significant regression (non-responders). The row maximum is shown in full yellow and row minimum is shown in full dark purple. Rows where statistically significant differences were calculated by one-way ANOVA test followed by pairwise comparisons are highlighted in red (Results were normalized to the means within each cytokine sub-column and are shown in percentage. 0% was defined as = 0 and 100% was defined as the largest mean in each data set). C. Blood serum was collected from mice when harvesting at the end of the experiments and analyzed using a 42-plex murine cytokine panel. Graph results of serum cytokine profiling of mice post treatment that show differential expression with statistical significance for partial responders to treatments verses non-responders. Analysis was done using the average of two technical replicates. Sample values that were above the upper limit of detection were recoded as the upper limit of detection; sample values that were below the lower limit of detection were recorded as 0 or a half of the lower limit of detection. *$P < 0.05$; **$P < 0.01$, by one-way ANOVA. D. Volcano plots illustrating the immune modulation of mouse serum cytokines. (a) Comparisons made between control and ONC201 treated groups. (b) Comparisons between enzalutamide and control groups. (c) Comparisons between darolutamide and control groups. (d) Comparisons between control group and the group treated with combination of ONC201 and enzalutamide. (e) Comparisons between control group and combination of ONC201 and darolutamide. Log2 (fold change) > 1 is indicated as upregulation (red), log2 (fold change) < 1 is indicated as downregulation (blue). Significance threshold used: $P < 0.05$.

of treatment effect (mean values ± SD) between the two groups yielded a statistically-significant increase in the following cytokines: GM-CSF (P = 0.0260), Chitinase-3-Like-1 (P = 0.0125), IL-2 (P = 0.0463), IFN-gamma (P = 0.0011), IL3 (P = 0.0098), CCL7/MCP-3/MARC (P = 0.0403), Prolactin (P = 0.0078), IL-1 alpha/IL-1F1 (0.0285), and MMP-12 (0.0472) (**Figure 9B** with red box highlights, **Figure 9C**). In **Figure 9D**, the volcano plot also displayed trends towards statistical significance in upregulation of pro-inflammatory and pro-apoptotic cytokines including CXCL/1/GRO alpha/KC/CINC-1 in the ONC201 treatment group (**Figure 9Da**), GDF-15, CCL7/MCP-3/MARC, CCL3/MIP-1alpha, CXCL1/GRO alpha/KC/CINC-1, IL-6 in the enzalutamide group (**Figure 9Db**), IL-17/IL-17A, MMP-8, GDF-15, and TWEAK/TNFSF12 in the darolutamide group (**Figure 9Dc**), Dkk-1 in the ONC201 and darolutamide combination group (**Figure 9De**), and IL-16 and IL-6 in the ONC201 and enzalutamide combination group (**Figure 9Dd**). Downregulation of IGF-1 in all treatment groups was observed. Other cytokines that exhibited trends of downregulation across the treatment groups include BAFF/Blys/TNFSF13B and VEGFR2/KDR/Flk-1. All comparisons in the volcano plot were relative to control group.

Taken together, the upregulation of pro-inflammatory cytokines promoting immune responses and downregulation of cytokines that promote growth factor or cell survival pathways may have contributed to the partial tumor regression seen in the experimental groups.

ONC206 shows strong synergy with enzalutamide, darolutamide or apalutamide in DU145 and PC3 prostate cancer cell lines

With previous experiments validating the anti-tumor efficacy of ONC201 and combinations of ONC201 and second generation NSAAs, it was hypothesized that ONC206, a more potent analogue of ONC201 that has shown preclinical pro-apoptotic effects in endometrial cancer [18], would yield better synergy with the new generation agents against prostate cancer. Two metastatic castration-resistant prostate cancer cell lines, DU145 and PC3 (**Table 1**) were used and treated with ONC206 and three second generation anti-androgen receptor signaling inhibitors enzalutamide, darolutamide, or apalutamide, as single agents or in combination with ONC206. Single agent dose-response curves were generated by the CTG cell viability assay, and IC50s for ONC206 (**Figure 10A**), enzalutamide (**Figure 2B**), darolutamide (**Figure 1**), and apalutamide (**Figure 10B**) were calculated. The CIs and heat maps indicating synergy or antagonism in the ONC206 and enzalutamide, darolutamide or apalutamide groups are shown (**Figure 10C**, **10D**; **Table 2**).

In vitro results indicate that both PC3 and DU145 cell lines are sensitive to ONC206 and strong synergy is observed in both PC3 and DU145 cell lines with the indicated combination therapies (**Figure 10C**, **10D**). An overall lower CI, shown for PC3 and DU145 (**Table 2**) was consistent with the hypothesis that ONC206 yields better synergy when combined with anti-androgen receptor signaling inhibitors in cell viability assays. The preliminary results with ONC206 support further studies using the indicated combination therapy *in vitro* and *in vivo* against advanced prostate cancer.

Sensitivity of 22RV1 in vivo to ONC201 and ONC201 plus darolutamide

Treatment with ONC201 at 50 or 100 mg/kg 3× per week demonstrates anti-tumor efficacy at the higher dose of ONC201 (**Figure 11A**). Because 100 mg/kg ONC201 is highly effective as monotherapy, we reduced the dose to 75 mg/kg and observed anti-tumor efficacy with the combination of ONC201 plus darolutamide *in vivo* (**Figure 11B**) and this was associated with increased TRAIL expression (**Figure 11C**). We did not observe alterations in ATF4, AR, or Ki67 in residual tumors.

Discussion

Our results provide a novel combination therapy using ONC201 or ONC206 and darolutamide as efficacious against human prostate cancer cells in culture. The combination of ONC201 and darolutamide shows therapeutic benefits in the 22RV1 castrate-resistant and androgen receptor signaling inhibitor-resistant *in vivo* xenograft model. Darolutamide has a favorable CNS toxicity profile vs enzalutamide and therefore would be a preferred choice for a human study in combination with ONC201 or ONC206 in prostate cancer.

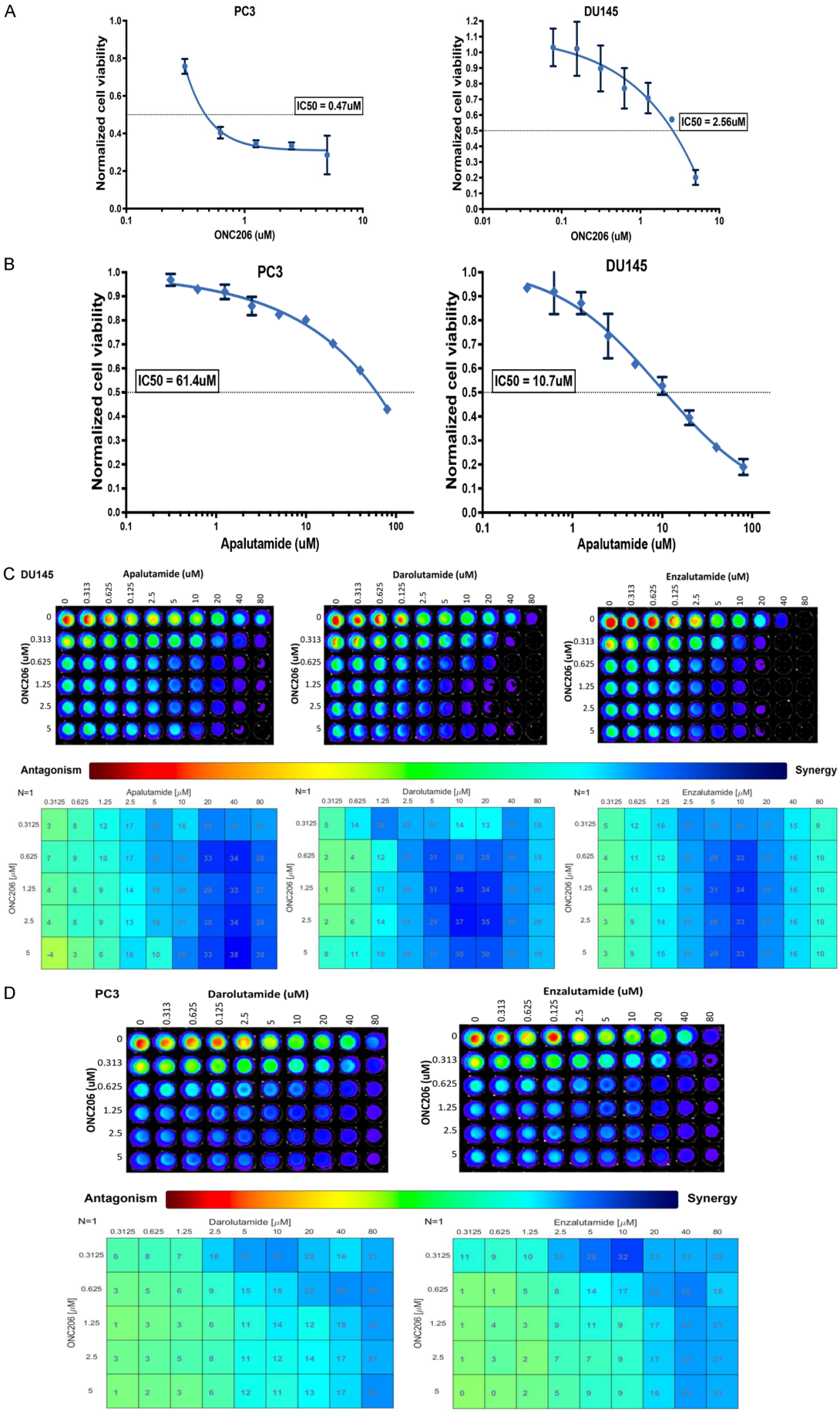
A
PC3
Normalized cell viability
IC50 = 0.47uM
ONC206 (uM)
DU145
IC50 = 2.56uM
B
PC3
IC50 = 61.4uM
Apalutamide (uM)
DU145
IC50 = 10.7uM
C DU145
Apalutamide (uM)
Darolutamide (uM)
Enzalutamide (uM)
ONC206 (uM)
Antagonism
Synergy
N=1
D
PC3
Darolutamide (uM)
Enzalutamide (uM)
ONC206 (uM)
Antagonism
Synergy
N=1

Figure 10. Representative dose-response curve and IC50s for ONC206 and apalutamide in two prostate cancer cell lines along with synergy analysis of ONC201 combination with enzalutamide, darolutamide or apalutamide. A. Pro-apoptotic and anti-proliferative effects measured using the CTG cell viability assay in PC3 and DU145 human prostate cancer cell lines at 72 hours post-treatment are shown. Representative dose-response curves and calculated IC50s of ONC206 for each prostate cancer cell line are shown. B. Pro-apoptotic and anti-proliferative effects measured using the CTG cell viability assay in PC3 and DU145 human prostate cancer cell lines at 72 hours post-treatment are shown. Representative dose-response curves and calculated IC50s for apalutamide in each prostate cancer cell line are shown. C. Combinations of ONC206 (0-5 μM), apalutamide (0-80 μM), darolutamide (0-80 μM) or enzalutamide (0-80 μM) were evaluated in DU145 human prostate cancer cell lines at 72 hours post treatment using the CTG cell viability assay. Synergistic doses are shown. D. Combinations of ONC206 (0-5 μM), darolutamide (0-80 μM) or enzalutamide (0-80 μM) were evaluated in PC3 human prostate cancer cells at 72 hours post-treatment using the CTG cell viability assay. Synergistic doses are shown.

Table 2. Representative CI-indices for combinations of ONC206 and anti-androgen receptor signaling inhibitory agents in DU145 and PC3 prostate cancer cell lines

DU145					Apalutamide					
5000/cells/well		0.313	0.625	1.25	2.5	5	10	20	40	80
ONC206	0.313	0.78	0.51	0.52	0.46	0.47	0.37	0.25	0.27	0.31
	0.625	0.26	0.17	0.21	0.16	0.20	0.19	0.17	0.19	0.02
	1.25	0.35	0.21	0.22	0.17	0.12	0.16	0.13	0.18	0.17
	2.5	0.73	0.45	0.32	0.21	0.18	0.19	0.17	0.18	0.23
	5	1.34	0.83	0.53	0.31	0.19	0.21	0.18	0.18	0.23
DU145					Darolutamide					
5000/cells/well		0.313	0.625	1.25	2.5	5	10	20	40	80
ONC206	0.313	1.29	0.85	0.65	0.50	0.42	0.55	0.28	0.28	0.21
	0.625	0.21	0.18	0.18	0.12	0.09	0.14	0.10	0.09	0.09
	1.25	0.40	0.33	0.29	0.21	0.14	0.18	0.13	0.11	0.11
	2.5	0.81	0.55	0.51	0.37	0.23	0.25	0.13	0.10	0.09
	5	3.11	1.68	0.52	0.57	0.96	0.26	0.12	0.06	0.06
DU145					Enzalutamide					
5000/cells/well		0.313	0.625	1.25	2.5	5	10	20	40	80
ONC206	0.313	0.78	0.51	0.52	0.46	0.47	0.37	0.25	0.27	0.31
	0.625	0.26	0.17	0.21	0.16	0.20	0.19	0.17	0.19	0.02
	1.25	0.35	0.21	0.22	0.17	0.12	0.16	0.13	0.18	0.17
	2.5	0.73	0.45	0.32	0.21	0.18	0.19	0.17	0.18	0.23
	5	1.34	0.83	0.53	0.31	0.19	0.21	0.18	0.18	0.23
PC3					Darolutamide					
5000/cells/well		0.313	0.625	1.25	2.5	5	10	20	40	80
ONC206	0.313	1.40	1.29	1.43	0.76	0.62	0.48	0.45	0.38	0.14
	0.625	0.43	0.39	0.37	0.31	0.21	0.21	0.16	0.15	0.05
	1.25	0.47	0.43	0.42	0.36	0.24	0.18	0.25	0.15	0.11
	2.5	0.78	0.74	0.65	0.54	0.40	0.39	0.33	0.26	0.16
	5	1.78	1.59	1.55	1.22	0.73	0.82	0.64	0.45	0.17
PC3					Enzalutamide					
5000/cells/well		0.313	0.625	1.25	2.5	5	10	20	40	80
ONC206	0.313	1.27	1.47	1.43	0.68	0.51	0.44	0.55	0.30	0.09
	0.625	0.33	0.35	0.27	0.22	0.16	0.15	0.12	0.15	0.17
	1.25	0.44	0.35	0.40	0.24	0.23	0.30	0.18	0.13	0.13
	2.5	0.85	0.73	0.84	0.53	0.57	0.52	0.27	0.18	0.14
	5	1.90	1.81	1.56	1.27	0.95	0.98	0.51	0.29	0.09

Highlights in yellow indicate synergy.

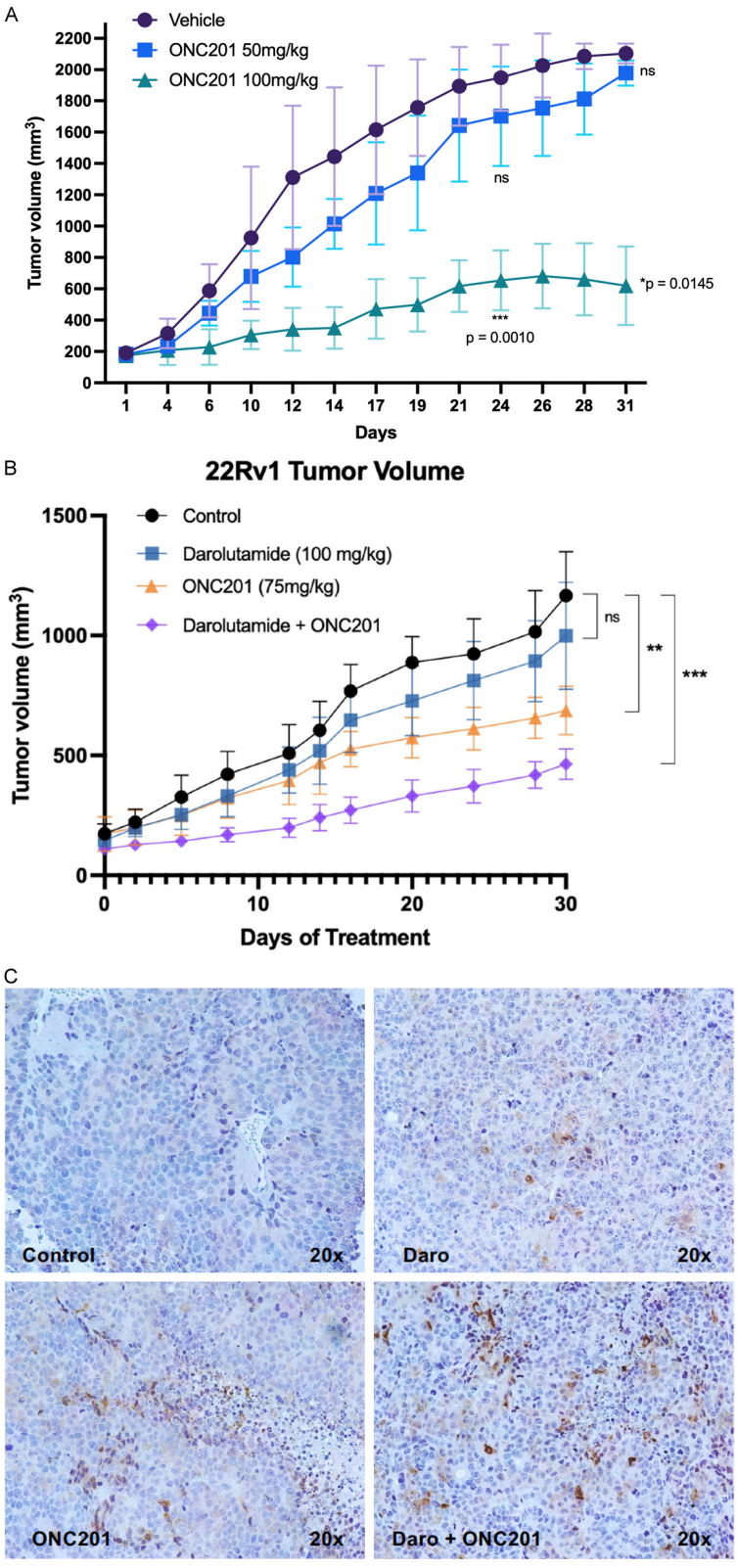

Figure 11. Growth of 22RV1 prostate cancer cells *in vivo*, anti-tumor efficacy using different doses of ONC201 alone or in combination with darolutamide along with increased TRAIL expression in tumor specimens. A. An initial experiment with varying doses of ONC201 *in vivo* to treat 22RV1 xenografts is shown. B. Tumor growth delay of 22RV1 xenografts *in vivo* in control mice, ONC201-treated mice (75 mg/kg), darolutamide-treated mice (100 mg/kg) or the combination of ONC201 plus darolutamide. C. Immunohistochemical stain for TRAIL protein expression in tumor xenografts is shown for the different treatment conditions.

The combination of ONC201 and both second generation NSAAs, enzalutamide or darolutamide, displayed anti-proliferative and pro-apoptotic effects in prostate cancer cells regardless of AR expression or castration sensitivity. We show that both nmCRPC and mCRPC cell lines are sensitive to darolutamide and that darolutamide alone decreases PSA level, induces ATF4, and downregulates AR activity in prostate cancer cell lines regardless of hormone sensitivity, AR status, or the presence of AR mutations.

We show that ONC201 reduces AR activity likely through the integrated stress response inhibiting protein translation and subsequently reduces PSA level as single agent in prostate cancer cells. While both ONC201 and darolutamide show ATF4 upregulation at 48 hours after treatment in the LNCaP cell line, significant reduction of PSA level is only observed in the combination groups. Since this occurs in the absence of PARP cleavage, hence no apoptotic activity, it was hypothesized that the induction of the ISR by the combination treatment and the competitive binding of darolutamide to the LBD of the AR collectively lead to significant reduction in PSA level. We tested this hypothesis by co-treating the PCa cells with 1 μg/mL DHT and the combination as well as single agent groups. Significant inhibition of AR activity was similarly

observed in both LNCaP and 22RV1 cell lines treated with the darolutamide and ONC201 combination.

Initial analysis of therapeutic benefits of combining ONC201 at 50 mg/kg on a weekly schedule and the anti-androgen receptor signaling agents in prostate cancer xenograft models *in vivo* showed no statistical significance although the combination of ONC201 and darolutamide showed trends of partial anti-tumor growth arrest as compared to the control group (especially after week 5 and towards the end of the six-week treatment period, demonstrated by reductions of final average tumor size (data not shown)). Given that in our previous study where ONC201 administered three-times per week with a dose of 50 mg/kg led to reduction in overall tumor sizes in both DU145 and PC3 xenograft models, the lack of robust anti-tumor effects with weekly ONC201 may be attributed to less frequent administration of the agent. We therefore tested 50 and 100 mg/kg ONC201 *in vivo* with 3× per week administration against 22RV1 xenografts and observed potent monotherapy effects with the 100 mg/kg dose. We therefore lowered the ONC201 dose to 75 mg/kg and observed *in vivo* synergy in combination with darolutamide.

Flow cytometric analysis showed trends of increased CD11b+ cells in treatment groups and TRAIL induction within NK cells after one week of treatment. The CD27 receptor is known to mediate the secretion of IFN-γ [31, 32], yielding the highest IFN-γ production in mature NK cells. Therefore, the trend of TRAIL upregulation seen could be induced by recruited intratumoral NK cells, demonstrating early drug-induced immune-modulation in the tumor microenvironment. Of note, a clear upregulation of the activating receptor NKp46 on the cell surface of peripheral blood NK cells (or homing NK cells) was observed in the ONC201 and darolutamide combination treatment group.

Although largely heterogenous, cytokine profiling results showed overall lower serum concentrations of tumorigenic cytokines IGF-1 and BAFF/Blys/TNFSF13B, and higher concentrations of immuno-modulatory cytokines such as IL-16, MMP8, TWEAK/TNFSF12 and Dkk-1. We then further divided the groups into partial-responders to treatments and non-responders to investigate the potential roles of NK cells in the tumors. Statistically significant higher concentrations of immuno-modulatory cytokines IFN-γ, GM-CSF, MMP-12, IL-1 alpha, IL-2, and IL-3 were observed in the partial-responders. However, little is known concerning the NK cell infiltration in the tumors. Additionally, due to the possession of several subsets, NK cells have shown both immuno-activating and immuno-tolerating behaviors that are dependent on the specific organ types and receptors in specialized conditions [33, 34]. Further analyses are required to investigate the potential NK cell anti-tumor activities *in vitro* and *in vivo*.

The findings from our study have several limitations that require further investigation. Despite the promising *in vitro* tissue culture results, our findings may not fully translate to the clinical setting due to the inherently limited environment of 2-D cell cultures. The *in vivo* experiments used a single xenograft model (22RV1), which may not represent the heterogeneity of human prostate cancer. Additionally, the short-term immune response data and small sample size limits the statistical significance and generalizability of the immune modulation observations. Heterogeneity in cytokine profiling complicates the interpretation of immune responses. While the combination of ONC201 and darolutamide demonstrated synergy, more comprehensive analyses are needed to fully understand the mechanisms underlying these effects, immune modulations, and therapeutic benefits. Optimal dosing regimens need to be determined, and the long-term efficacy and safety of the combination therapy were not thoroughly explored, warranting further investigation. Future directions also include comprehensive translational and human clinical studies, which are necessary to validate these pre-clinical findings and establish the efficacy and safety of the combination therapy in treating advanced or metastatic prostate cancer.

In summary, our present studies demonstrate a novel synergistic combination using ONC201 or ONC206 and darolutamide in pre-clinical treatment for prostate cancer. Cell culture data demonstrate significant drug sensitivity and synergistic anti-tumor efficacy in both metastatic and non-metastatic prostate cancer cell lines regardless of castration sensitivity and AR status. Synergistic effects are observed in AR-negative cell lines, such as PC3 and DU145.

In vivo experiments using 22RV1 CRPC cells with an optimized treatment and dosing regimen demonstrate therapeutic benefits of the combination of ONC201 plus darolutamide therapy and role of immune modulation of NK cells against advanced prostate cancer in mice. To date in 2024, there has not been a phase II clinical study of ONC201 in prostate cancer and no phase 1b/II clinical study of ONC201 plus anti-androgen receptor signaling blockade in castrate-resistant prostate cancer. Conducting such a study in humans would allow the preclinical advances to be translated for potential patient benefit. Our results warrant further translational and clinical studies with imipridones ONC201/ONC201 or ONC201/ONC206 in combination with enzalutamide or darolutamide for treatment of castrate resistant advanced or metastatic prostate cancer.

Acknowledgements

W.S.E-D. is an American Cancer Society Research Professor and is supported by the Mencoff Family University Professorship at Brown University. This work was supported by an NIH grant (CA173453) to W.S.E-D. This work was presented in part at the 2022 meeting of the American Association for Cancer Research.

Disclosure of conflict of interest

W.S.E-D. is a co-founder of Oncoceutics, Inc., a subsidiary of Chimerix. Dr. El-Deiry has disclosed his relationship with Oncoceutics/Chimerix and potential conflict of interest to his academic institution/employer and is fully compliant with NIH and institutional policy that is managing this potential conflict of interest.

Address correspondence to: Wafik S El-Deiry, Laboratory of Translational Oncology and Experimental Cancer Therapeutics, The Warren Alpert Medical School, Brown University, Providence, RI 02903, USA. E-mail: wafik@brown.edu

References

[1] Cai M, Song XL, Li XA, Chen M, Guo J, Yang DH, Chen Z and Zhao SC. Current therapy and drug resistance in metastatic castration-resistant prostate cancer. Drug Resist Updat 2023; 68: 100962.

[2] Le TK, Duong QH, Baylot V, Fargette C, Baboudjian M, Colleaux L, Taieb D and Rocchi P. Castration-resistant prostate cancer: from uncovered resistance mechanisms to current treatments. Cancers (Basel) 2023; 15: 5047.

[3] Sumanasuriya S and De Bono J. Treatment of advanced prostate cancer-a review of current therapies and future promise. Cold Spring Harb Perspect Med 2018; 8: a030635.

[4] Posdzich P, Darr C, Hilser T, Wahl M, Herrmann K, Hadaschik B and Grünwald V. Metastatic prostate cancer-a review of current treatment options and promising new approaches. Cancers (Basel) 2023; 15: 461.

[5] James ND, de Bono JS, Spears MR, Clarke NW, Mason MD, Dearnaley DP, Ritchie AWS, Amos CL, Gilson C, Jones RJ, Matheson D, Millman R, Attard G, Chowdhury S, Cross WR, Gillessen S, Parker CC, Russell JM, Berthold DR, Brawley C, Adab F, Aung S, Birtle AJ, Bowen J, Brock S, Chakraborti P, Ferguson C, Gale J, Gray E, Hingorani M, Hoskin PJ, Lester JF, Malik ZI, McKinna F, McPhail N, Money-Kyrle J, O'Sullivan J, Parikh O, Protheroe A, Robinson A, Srihari NN, Thomas C, Wagstaff J, Wylie J, Zarkar A, Parmar MKB and Sydes MR; STAMPEDE Investigators. Abiraterone for prostate cancer not previously treated with hormone therapy. N Engl J Med 2017; 377: 338-351.

[6] Davis ID, Martin AJ, Stockler MR, Begbie S, Chi KN, Chowdhury S, Coskinas X, Frydenberg M, Hague WE, Horvath LG, Joshua AM, Lawrence NJ, Marx G, McCaffrey J, McDermott R, McJannett M, North SA, Parnis F, Parulekar W, Pook DW, Reaume MN, Sandhu SK, Tan A, Tan TH, Thomson A, Tu E, Vera-Badillo F, Williams SG, Yip S, Zhang AY, Zielinski RR and Sweeney CJ; ENZAMET Trial Investigators and the Australian and New Zealand Urogenital and Prostate Cancer Trials Group. Enzalutamide with standard first-line therapy in metastatic prostate cancer. N Engl J Med 2019; 381: 121-131.

[7] Smith MR, Hussain M, Saad F, Fizazi K, Sternberg CN, Crawford ED, Kopyltsov E, Park CH, Alekseev B, Montesa-Pino A, Ye D, Parnis F, Cruz F, Tammela TLJ, Suzuki H, Utriainen T, Fu C, Uemura M, Méndez-Vidal MJ, Maughan BL, Joensuu H, Thiele S, Li R, Kuss I and Tombal B; ARASENS Trial Investigators. Darolutamide and survival in metastatic, hormone-sensitive prostate cancer. N Engl J Med 2022; 386: 1132-1142.

[8] Kensler KH, Baichoo S, Pathania S and Rebbeck TR. The tumor mutational landscape of BRCA2-deficient primary and metastatic prostate cancer. NPJ Precis Oncol 2022; 6: 39.

[9] Cotter K and Rubin MA. The evolving landscape of prostate cancer somatic mutations. Prostate 2022; 82 Suppl 1: S13-S24.

[10] van Dessel LF, van Riet J, Smits M, Zhu Y, Hamberg P, van der Heijden MS, Bergman AM, van Oort IM, de Wit R, Voest EE, Steeghs N, Yamaguchi TN, Livingstone J, Boutros PC, Martens JWM, Sleijfer S, Cuppen E, Zwart W, van de Werken HJG, Mehra N and Lolkema MP. The genomic landscape of metastatic castration-resistant prostate cancers reveals multiple distinct genotypes with potential clinical impact. Nat Commun 2019; 10: 5251.

[11] Conteduca V, Oromendia C, Eng KW, Bareja R, Sigouros M, Molina A, Faltas BM, Sboner A, Mosquera JM, Elemento O, Nanus DM, Tagawa ST, Ballman KV and Beltran H. Clinical features of neuroendocrine prostate cancer. Eur J Cancer 2019; 121: 7-18.

[12] Alabi BR, Liu S and Stoyanova T. Current and emerging therapies for neuroendocrine prostate cancer. Pharmacol Ther 2022; 238: 108255.

[13] Karzai F and Madan RA. Deciphering the enigma of neuroendocrine prostate cancer. J Clin Invest 2022; 132: e164611.

[14] Saini S, Sreekumar A, Nathani S, Asante DM and Simmons MN. A novel exosome based therapeutic intervention against neuroendocrine prostate cancer. Sci Rep 2024; 14: 2816.

[15] Wang Y, Wang Y, Ci X, Choi SYC, Crea F, Lin D and Wang Y. Molecular events in neuroendocrine prostate cancer development. Nat Rev Urol 2021; 18: 581-596.

[16] Liang H, Liu Y, Guo J, Dou M, Zhang X, Hu L and Chen J. Progression in immunotherapy for advanced prostate cancer. Front Oncol 2023; 13: 1126752.

[17] Allen JE, Krigsfeld G, Mayes PA, Patel L, Dicker DT, Patel AS, Dolloff NG, Messaris E, Scata KA, Wang W, Zhou JY, Wu GS and El-Deiry WS. Dual inactivation of Akt and ERK by TIC10 signals Foxo3a nuclear translocation, TRAIL gene induction, and potent antitumor effects. Sci Transl Med 2013; 5: 171ra17.

[18] Stein MN, Bertino JR, Kaufman HL, Mayer T, Moss R, Silk A, Chan N, Malhotra J, Rodriguez L, Aisner J, Aiken RD, Haffty BG, DiPaola RS, Saunders T, Zloza A, Damare S, Beckett Y, Yu B, Najmi S, Gabel C, Dickerson S, Zheng L, El-Deiry WS, Allen JE, Stogniew M, Oster W and Mehnert JM. First-in-human clinical trial of oral ONC201 in patients with refractory solid tumors. Clin Cancer Res 2017; 23: 4163-4169.

[19] Arrillaga-Romany I, Gardner SL, Odia Y, Aguilera D, Allen JE, Batchelor T, Butowski N, Chen C, Cloughesy T, Cluster A, de Groot J, Dixit KS, Graber JJ, Haggiagi AM, Harrison RA, Kheradpour A, Kilburn LB, Kurz SC, Lu G, MacDonald TJ, Mehta M, Melemed AS, Nghiemphu PL, Ramage SC, Shonka N, Sumrall A, Tarapore RS, Taylor L, Umemura Y and Wen PY. ONC201 (Dordaviprone) in recurrent H3 K27M-mutant diffuse midline glioma. J Clin Oncol 2024; 42: 1542-1552.

[20] Venneti S, Kawakibi AR, Ji S, Waszak SM, Sweha SR, Mota M, Pun M, Deogharkar A, Chung C, Tarapore RS, Ramage S, Chi A, Wen PY, Arrillaga-Romany I, Batchelor TT, Butowski NA, Sumrall A, Shonka N, Harrison RA, de Groot J, Mehta M, Hall MD, Daghistani D, Cloughesy TF, Ellingson BM, Beccaria K, Varlet P, Kim MM, Umemura Y, Garton H, Franson A, Schwartz J, Jain R, Kachman M, Baum H, Burant CF, Mottl SL, Cartaxo RT, John V, Messinger D, Qin T, Peterson E, Sajjakulnukit P, Ravi K, Waugh A, Walling D, Ding Y, Xia Z, Schwendeman A, Hawes D, Yang F, Judkins AR, Wahl D, Lyssiotis CA, de la Nava D, Alonso MM, Eze A, Spitzer J, Schmidt SV, Duchatel RJ, Dun MD, Cain JE, Jiang L, Stopka SA, Baquer G, Regan MS, Filbin MG, Agar NYR, Zhao L, Kumar-Sinha C, Mody R, Chinnaiyan A, Kurokawa R, Pratt D, Yadav VN, Grill J, Kline C, Mueller S, Resnick A, Nazarian J, Allen JE, Odia Y, Gardner SL and Koschmann C. Clinical efficacy of ONC201 in H3K27M-mutant diffuse midline gliomas is driven by disruption of integrated metabolic and epigenetic pathways. Cancer Discov 2023; 13: 2370-2393.

[21] Arrillaga-Romany I, Lassman A, McGovern SL, Mueller S, Nabors B, van den Bent M, Vogelbaum MA, Allen JE, Melemed AS, Tarapore RS, Wen PY and Cloughesy T. ACTION: a randomized phase 3 study of ONC201 (dordaviprone) in patients with newly diagnosed H3 K27M-mutant diffuse glioma. Neuro Oncol 2024; 26: S173-S181.

[22] Stein MN, Malhotra J, Tarapore RS, Malhotra U, Silk AW, Chan N, Rodriguez L, Aisner J, Aiken RD, Mayer T, Haffty BG, Newman JH, Aspromonte SM, Bommareddy PK, Estupinian R, Chesson CB, Sadimin ET, Li S, Medina DJ, Saunders T, Frankel M, Kareddula A, Damare S, Wesolowsky E, Gabel C, El-Deiry WS, Prabhu VV, Allen JE, Stogniew M, Oster W, Bertino JR, Libutti SK, Mehnert JM and Zloza A. Safety and enhanced immunostimulatory activity of the DRD2 antagonist ONC201 in advanced solid tumor patients with weekly oral administration. J Immunother Cancer 2019; 7: 136.

[23] Wagner J, Kline CL, Zhou L, Campbell KS, MacFarlane AW, Olszanski AJ, Cai KQ, Hensley HH, Ross EA, Ralff MD, Zloza A, Chesson CB, Newman JH, Kaufman H, Bertino J, Stein M and El-Deiry WS. Dose intensification of TRAIL-inducing ONC201 inhibits metastasis and promotes intratumoral NK cell recruitment. J Clin Invest 2018; 128: 2325-2338.

[24] Lev A, Lulla AR, Ross BC, Ralff MD, Makhov PB, Dicker DT and El-Deiry WS. ONC201 targets AR

and AR-V7 signaling, reduces PSA, and synergizes with everolimus in prostate cancer. Mol Cancer Res 2018; 16: 754-766.
[25] Anderson PM, Trucco MM, Tarapore RS, Zahler S, Thomas S, Gortz J, Mian O, Stoignew M, Prabhu V, Morrow S and Allen JE. Phase II study of ONC201 in neuroendocrine tumors including pheochromocytoma-paraganglioma and desmoplastic small round cell tumor. Clin Cancer Res 2022; 28: 1773-1782.
[26] Bastos DA and Antonarakis ES. Darolutamide for castration-resistant prostate cancer. Onco Targets Ther 2019; 12: 8769-8777.
[27] Moilanen AM, Riikonen R, Oksala R, Ravanti L, Aho E, Wohlfahrt G, Nykänen PS, Törmäkangas OP, Palvimo JJ and Kallio PJ. Discovery of ODM-201, a new-generation androgen receptor inhibitor targeting resistance mechanisms to androgen signaling-directed prostate cancer therapies. Sci Rep 2015; 5: 12007.
[28] El-Amm J, Patel N, Freeman A and Aragon-Ching JB. Metastatic castration-resistant prostate cancer: critical review of enzalutamide. Clin Med Insights Oncol 2013; 7: 235-245.
[29] Claessens F, Helsen C, Prekovic S, Van den Broeck T, Spans L, Van Poppel H and Joniau S. Emerging mechanisms of enzalutamide resistance in prostate cancer. Nat Rev Urol 2014; 11: 712-716.
[30] Pignon JC, Koopmansch B, Nolens G, Delacroix L, Waltregny D and Winkler R. Androgen receptor controls EGFR and ERBB2 gene expression at different levels in prostate cancer cell lines. Cancer Res 2009; 69: 2941-2949.
[31] Michel T, Poli A, Domingues O, Mauffray M, Thérésine M, Brons NH, Hentges F and Zimmer J. Mouse lung and spleen natural killer cells have phenotypic and functional differences, in part influenced by macrophages. PLoS One 2012; 7: e51230.
[32] Hayakawa Y and Smyth MJ. CD27 dissects mature NK cells into two subsets with distinct responsiveness and migratory capacity. J Immunol 2006; 176: 1517-1524.
[33] Vivier E, Nunès JA and Vély F. Natural killer cell signaling pathways. Science 2004; 306: 1517-1519.
[34] Grégoire C, Chasson L, Luci C, Tomasello E, Geissmann F, Vivier E and Walzer T. The trafficking of natural killer cells. Immunol Rev 2007; 220: 169-182.
[35] Sramkoski RM, Pretlow TG 2nd, Giaconia JM, Pretlow TP, Schwartz S, Sy MS, Marengo SR, Rhim JS, Zhang D and Jacobberger JW. A new human prostate carcinoma cell line, 22Rv1. In Vitro Cell Dev Biol Anim 1999; 35: 403-409.
[36] Horoszewicz JS, Leong SS, Kawinski E, Karr JP, Rosenthal H, Chu TM, Mirand EA and Murphy GP. LNCaP model of human prostatic carcinoma. Cancer Res 1983; 43: 1809-1818.
[37] Stone KR, Mickey DD, Wunderli H, Mickey GH and Paulson DF. Isolation of a human prostate carcinoma cell line (DU 145). Int J Cancer 1978; 21: 274-281.
[38] Kaighn ME, Narayan KS, Ohnuki Y, Lechner JF and Jones LW. Establishment and characterization of a human prostatic carcinoma cell line (PC-3). Invest Urol 1979; 17: 16-23.